

7

ENSO Irregularity and Asymmetry

Soon-Il An¹, Eli Tziperman², Yuko M. Okumura³, and Tim Li⁴

ABSTRACT

The El Niño Southern Oscillation (ENSO) is characterized by being irregular or nonperiodic and asymmetric between El Niño and La Niña with respect to amplitude, pattern, and temporal evolution. These observed features suggest the importance of nonlinear dynamics and/or stochastic forcing. Both nonlinear deterministic chaos and linear dynamics subject to stochastic forcing and/or to non-normal growth were introduced to explain the irregularity of ENSO, but no consensus has been reached to date given the short observational record. As a dominant source of stochastic forcing, westerly wind bursts play a role in triggering, amplifying, and determining the irregularity and asymmetry of ENSO, which are best treated as part of the deterministic dynamics or as a multiplicative noise forcing. Various nonlinear processes are responsible for the spatial and temporal asymmetry of El Niño and La Niña, which includes nonlinear ocean advection, nonlinear atmosphere-ocean coupling, state-dependent stochastic noise, tropical instability waves, and biophysical processes. In addition to the internal nonlinear processes, a capacitor effect of the Indian and Atlantic Oceans and atmospheric and oceanic teleconnections from extratropical Pacific could also contribute to the temporal and amplitude asymmetry of ENSO. Despite significant progress, most state-of-the-art models are still lacking in simulation of the spatial and temporal asymmetry of ENSO.

7.1. INTRODUCTION

The irregularity of the El Niño Southern Oscillation (ENSO), including its amplitude, interval between events, and spatial and temporal patterns, has been explained as being either a result of large-scale deterministic nonlinear dynamics or the result of stochastic forcing, although these theories are not mutually exclusive. In the first case, the irregularity is due to jumping between nonlinear res-

onances of the ENSO cycle and the seasonal cycle (Tziperman et al., 1994, 1995; Jin et al., 1994; Chang et al., 1994; An & Jin, 2011). This theory can also account for the tendency of El Niño to peak at the end of the calendar year, explaining it through phase locking to the annual cycle (above references). Yet Stein et al. (2010, 2011) employed seasonally modulated linear dynamics under stochastic forcing and found phase locking as well, indicating that nonlinear dynamics may not be necessary for explaining ENSO's seasonality. In the second case, stochastic variability, representing for example short-term weather events, leads to the irregularity of ENSO, potentially also amplified by non-normal transient growth (e.g., Moore & Kleeman, 1999; Penland & Sardeshmukh, 1995).

Since the observational record of tropical Pacific SST is still not long enough to distinguish between these two scenarios, no consensus on this matter has been reached (Kessler, 2002). Tropical climate state is a primary factor to

¹Department of Atmospheric Sciences, Yonsei University, Seoul, Republic of Korea

²Department of Earth and Planetary Sciences and School of Engineering and Applied Sciences, Harvard University, Cambridge, MA, USA

³Institute for Geophysics, Jackson School of Geosciences, The University of Texas at Austin, Austin, TX, USA

⁴Department of Atmospheric Sciences/IPRC, University of Hawai'i at Mānoa, Honolulu, HI, USA

determine an atmosphere-ocean coupled stability for ENSO system (T. Li, 1997b; An & Jin, 2000; Fedorov & Philander, 2000), and for example, depending on the coupling strength, ENSO system becomes a self-sustained and possibly chaotic oscillator under a strong coupling and a damped oscillator under a weak coupling (An & Jin, 2001). It has been suggested that some decades may be characterized by a self-sustained, possibly chaotic dynamics, while others show a damped ENSO cycle, excited by stochastic variability (Kirtman & Schopf, 1998). However, a bifurcation between stable and unstable regimes tends to be ambiguous in the presence of noise (e.g., Levine & Jin, 2010).

Westerly wind bursts (WWBs) are episodic reversals of the equatorial trade winds with a strength of 5 to 7 ms^{-1} , zonal extent of 20–40 degrees, duration of 5–30 days, and frequency of around 5 to 10 times per year (Harrison & Vecchi, 1997; L. Yu et al., 2003; Seiki & Takayabu, 2007a). These events, a dominant source of stochastic forcing, play a role in triggering, amplifying, and even determining the spatial pattern of ENSO events (Harrison & Vecchi, 1997; Eisenman et al., 2005; Levine & Jin, 2010; Rong et al., 2011; D. Chen et al., 2015; Hayashi & Watanabe, 2017). WWBs were initially considered as additive stochastic forcing (e.g. Moore & Kleeman, 1999), yet it became clear that they depend on the background SST and tend to occur more frequently during a developing El Niño (Verbickas, 1998; L. Yu et al., 2003; Eisenman et al., 2005). These events are thus best treated as part of the deterministic dynamics or as a state-dependent multiplicative noise forcing, with important implications to amplitude and predictability of El Niño events.

El Niño is not a simple mirror image of its opposite phase, La Niña. El Niño's amplitude is on average greater than that of La Niña (Deser & Wallace, 1987; Burgers & Tephenson, 1999; An & Jin, 2004). El Niño is often followed by a La Niña in the following year, but the opposite is much less common (Larkin & Harrison, 2002; M. Chen et al., 2016; An & Kim, 2017). After their mature phase, many La Niñas persist through the following year, but most of El Niños tend to decay rapidly by next summer (Ohba & Ueda, 2007; Okumura & Deser, 2010; Choi et al. 2013; DiNezio & Deser, 2014; An & Kim, 2018). Strong El Niños are mainly loaded over the eastern Pacific with focusing toward the equator, whereas strong La Niñas are mostly loaded over the central Pacific with a wider latitudinal extension (Hoerling et al., 1997; Kang & Kug, 2002; Takahashi et al., 2011; Dommenges et al., 2013). Such amplitude/duration/transition/pattern asymmetries between El Niño and La Niña may not be surprising given the nonlinear internal dynamics and/or selective external impacts (e.g., An & Kim, 2018). Asymmetrical internal nonlinear processes that are responsible for amplitude asymmetry include the vertical ocean temperature profile (Zebiak & Cane, 1986), ocean nonlinear advection (An &

Jin, 2004; Su et al. 2010), asymmetric equatorial wind response to SST (Kang & Kug, 2002; Frauen & Dommenges, 2010; Choi et al., 2013), ocean wave response to the wind stress (An & Kim, 2017, 2018), outcropping thermocline nonlinearity (Battisti & Hirst, 1989; Galanti et al., 2002; An & Jin, 2004), state-dependent stochastic forcing (Jin et al., 2007; Kug et al., 2008; Rong et al., 2011; Levine et al., 2016; Hayashi & Watanabe, 2017), tropical instability wave activity (J. Yu & Liu, 2003; An, 2008a, 2008b), biophysical feedback (Timmermann & Jin, 2002), shortwave feedback (Lloyd et al., 2012), etc. Transition/duration asymmetry has been attributed to a selective capacitor effect of the Indian and Atlantic oceans (Ohba & Ueda, 2007; Okumura & Deser, 2010; An & Kim, 2018), development of subtropical western Pacific atmospheric circulation during decaying phase of ENSO to boost ENSO transition (B. Wang et al., 1999; B. Wang et al., 2001; Y. Li et al., 2007; B. Wu et al., 2010a), and some of aforementioned internal nonlinear processes (Choi et al., 2013; Im et al., 2015; M. Chen et al., 2016; An & Kim, 2017, 2018; M. Chen & Li, 2018).

This chapter focuses on the irregularity of ENSO and on its amplitude and evolution asymmetries. In section 7.2, the origin of irregularity will be addressed together with the role of westerly wind burst events. Mechanisms for amplitude asymmetry will be discussed in section 7.3. The cause of evolution asymmetry will be reviewed in section 7.4, and we include conclusion and discussion in section 7.5.

7.2. IRREGULARITY

7.2.1. Deterministic Chaos

A dynamical system can display chaotic behavior without any external stochastic forcing, the most well-known example of this being the three nonlinear ordinary differential equations of the Lorenz system (Lorenz, 1963). It has been suggested that the irregularity of ENSO, including its amplitude, interval between events, and spatial and temporal patterns, may be a result of such deterministic large-scale nonlinear dynamics (Tziperman et al., 1994; Jin et al., 1994). Chaotic dynamical systems are typically characterized via the “route to chaos” they undergo as a parameter is changed. There are three possibilities (Strogatz, 1994; Ott, 2002): the period doubling route, the intermittency route, and the quasi-periodicity route to chaos. This last route is typical of periodically forced nonlinear oscillators and is the relevant one in the case of ENSO, where the periodic forcing is provided by the seasonal cycle and the nonlinear oscillator is ENSO itself.

When the periodic forcing (seasonal cycle in the case of ENSO) is weak, the nonlinear oscillator undergoes

oscillation at a frequency that is not simply related to the forcing frequency. This is known as the quasi-periodic regime. As the periodic forcing amplitude is increased, the forced nonlinear oscillator can enter a nonlinear resonance with the forcing when the ratio of its frequency and that of the forcing is that of two integers, p/q . Unlike a linear oscillator, a nonlinear one can adjust its period as function of its amplitude, and thus may be in more than a single nonlinear resonance with the given periodic forcing. When the nonlinearity is even stronger, these different nonlinear resonances may coexist for exactly the same parameters, and the resonances can then become unstable. That is, there would be a solution for ENSO that is perfectly periodic, with a period of, say 3 years (3/1 resonance), and another such solution with a period of 4 years (4/1 resonance), with the actual solution and thus the period determined by the initial conditions. In this strongly nonlinear/strongly forced regime, these solutions are unstable, so that any slight deviation from the periodic solution (due to error in the initial conditions or due to finite accuracy in the calculation of the solution), would grow exponentially fast and the solution may then switch to another nonlinear resonance and thus to a different periodicity. This would lead to random jumping between these nonlinear resonances and thus to a chaotic solution with a limited predictability and irregular period and amplitude.

This mechanism for ENSO's irregularity has been demonstrated in the context of various simple toy models (Tziperman et al., 1994; Jin et al., 1994; Chang et al., 1994; An & Jin, 2011) as well as in the Cane-Zebiak Model (Zebiak & Cane, 1987) that was the first dynamical model to be used successfully for ENSO prediction (Cane et al., 1986). Figure 7.1 shows the three regimes for the CZ model: quasi-periodic (left), phase-locked nonlinear resonance (middle; note in lower panel that all events occur only in January and February in this case) and chaotic (right, where events happen throughout the year, yet preferentially at the end and beginning of the calendar year). Note that "phase locking" is strictly defined as the period of ENSO being related to that of the annual cycle as the ratio of two integers p/q . In the chaotic regime, though, we use the term more loosely to denote a preferential occurrence of warm events during a certain season. The quasi-periodicity route to chaos can be seen in these models by varying the amplitude of the seasonal cycle or of the ocean-atmosphere coupling, for example. As the seasonal cycle amplitude is increased, ENSO is seen to first be in a periodic solution that is not associated with the seasonal cycle, then for stronger seasonal forcing it enters a nonlinear resonance with the seasonal cycle such that its period is p/q times one year. Eventually, for even stronger forcing, the ENSO cycle becomes chaotic. An & Jin (2011) showed that the frequency modulation by the annual cycle can change

ENSO's phases and frequency, while the amplitude modulation by the annual cycle intensifies the ENSO variability and also induces seasonal amplitude locking.

When ENSO is in a nonlinear resonance with the seasonal cycle it is phased locked to this cycle. If the resonance were $p/q = 4/1$, for example, ENSO would always occur at the same season, every four years. In the chaotic regime, the different resonances would still tend to be phase locked and ENSO would still tend to preferentially occur at a given season. This is reminiscent of the known locking of El Niño events to the annual cycle, adding to the attractiveness of the deterministic chaos explanation for ENSO's irregularity and phase locking (above references, as well as Stein et al., 2010, 2011). This still leaves open the question of what precisely is the mechanism of the phase locking, and some attempts on that were made by noting the possible seasonal amplification of the different equatorial wave modes (Tziperman et al., 1997; Galanti & Tziperman, 2000) as well as via a cloud feedback (Dommenges & Yu, 2016). Similarly, ENSO termination time was suggested to be determined by the southward migration of westerly wind anomalies from the equator associated with climatological warm pool expansion (Vecchi, 2006; McGregor et al., 2012), or by the development of an anomalous western North Pacific anticyclone (B. Wang et al., 2000; Stuecker et al., 2013). Future work will need to attempt to identify specific evidence for the nonlinear resonances involving the seasonal cycle. This may need to be done using very long integrations of state-of-the-art general circulation models that allow separating the effects of small nonlinearities from weather noise. Simpler models that have been used to study these issues are useful mostly in suggesting hypotheses but not in testing their realism.

7.2.2. Stochastic Forcing

Weather variability, although deterministic, has a much shorter timescale than that of ENSO, allowing us to treat it as noise, or stochastic forcing. The solution to a simple linear dynamical system $dx/dt = Ax$, where $\mathbf{x}(t)$ is a vector (say SST or thermocline depth at a set of grid points covering the tropical Pacific), and A a matrix, would ultimately decay if the eigenvalues of A all have negative real parts. However, if the matrix A is non-normal, that is, if $AA^T \neq A^T A$, its eigenvectors are not orthogonal and then $\mathbf{x}(t)$ may display potentially large growth before decaying (Farrell, 1988; Farrell & Ioannou, 1996). The initial conditions $\mathbf{x}(t = 0)$ of a unit norm, $|\mathbf{x}(t = 0)| = 1$, leading to this non-normal growth are known as optimal initial conditions. Such optimal initial conditions may be excited by noise and then amplified by non-normal growth. It has been suggested that the warming during El Niño events is due to such non-normal growth (e.g. Moore & Kleeman, 1999; Penland & Sardeshmukh, 1995).

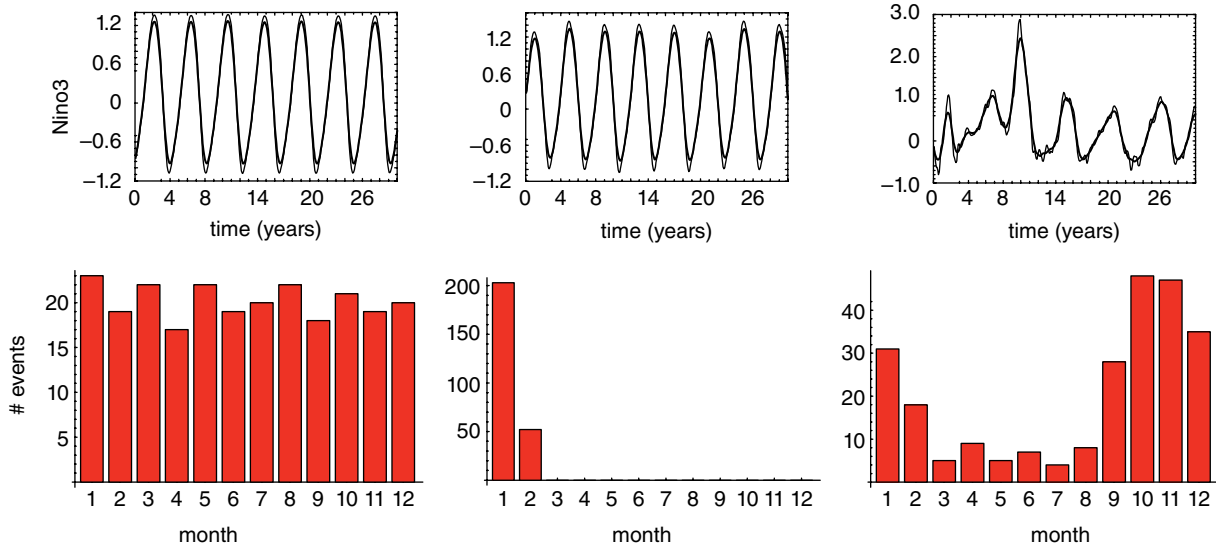


Figure 7.1 Transition to chaos of the CZ model as the seasonal forcing is increased. Upper panels: time series of the model Niño-3 index, lower panels: histogram of number of warm events per month. Left: quasi-periodic regime obtained for perpetual July background state (no seasonal cycle), with a period of about 4.3 years that is not simply related to the annual cycle. Middle: phase-locked regime, obtained for weak seasonality (background seasonality amplitude set to 0.2 times the standard), very nearly 4-year period. Right: chaotic regime in the standard parameter with a full-amplitude seasonal cycle.

Since the observational record of tropical Pacific SST is not sufficiently long to distinguish between the chaotic deterministic dynamics and stochastically driven random scenarios for ENSO's irregularity, no consensus on this matter has been reached (Kessler, 2002). The tropical climate background state determines the atmosphere-ocean coupled stability for ENSO (An & Jin, 2000; Fedorov & Philander, 2000), which can put ENSO in a self-sustained and possibly chaotic regime under a strong coupling and a damped oscillator under a weak coupling. It has been suggested that some decades may be characterized by self-sustained, possibly chaotic dynamics, while others show a damped ENSO cycle, excited by stochastic variability (Kirtman & Schopf, 1998). This is further complicated by the presence of noise, as a bifurcation between stable and unstable regimes tends to be ambiguous then (e.g., Stone et al., 1998; Levine & Jin, 2010). Verification using fully-coupled general circulation models is complicated by the presence of weather noise in these models. In principle, it is possible to differentiate between irregularity due to weather noise and large-scale nonlinear dynamics by examining the fractal dimension of the motion (Tziperman et al., 1994), yet this is complicated by the need to run the model for very long periods in order to reliably estimate the dimension, which is challenging for computationally expensive state-of-the-art general circulation models. Finally, we note that non-normal dynamics can play an important role in a purely deterministic and chaotic ENSO regime as well (Samelson & Tziperman, 2001).

7.2.3. Role and Dynamics of WWBs as State-Dependent ENSO Forcing

WWBs trigger Kelvin waves that play a significant role in ENSO events (McPhaden et al., 1992; Kessler et al., 1995; Levine & Jin, 2010; D. Chen et al., 2015; Hayashi & Watanabe, 2017). Due to their short timescale, WWBs were initially considered as additive stochastic forcing (e.g. Moore & Kleeman, 1999). To analyze this, consider a stochastically driven set of linear ordinary differential equations, $dx/dt = Ax + \xi v(t)$, where ξ is a constant unit norm vector, $|\xi| = 1$, and $v(t)$ is a scalar stochastic forcing, say a gaussian white noise. One may now calculate the “stochastic optimals,” that is, the shape of ξ that leads to the maximum variance of $x(t)$. It has been suggested by the above references that WWBs have a shape that is close to the stochastic optimals for ENSO, or that they excite anomalies (say in thermocline depth or SST) that are close to the optimal initial conditions that lead to strong El Niño growth. This would make WWBs an especially powerful stochastic forcing of ENSO.

Yet it became clear that these events that strongly depend on the state of the SST tend to occur much more frequently during an already developing El Niño (Verbickas, 1998; L. Yu et al., 2003). That is, these events cannot be seen as a purely random wind forcing that is then amplified by the Bjerknes feedback. Instead, the occurrence of these events, as well as their location, scale, amplitude, and duration, while having a stochastic

element, all strongly depend on the developing SST of warm events (Tziperman & Yu, 2007). These events are thus best treated as part of the deterministic dynamics. The SST dependence of WWBs means that rather than being an additive random forcing, they can be thought of as being “multiplicative random forcing” (e.g. Perez et al., 2005; Jin et al., 2007). The dependence of WWB probability of occurrence, amplitude, scale etc., on the SST has important implications to the amplitude and predictability of El Niño events (Eisenman et al., 2005). The SST dependence of the WWB characteristics can be extracted using SVD analysis of the covariance matrix between these characteristics and the SST (Tziperman & Yu, 2007), and this allows to parameterize WWBs in ENSO models whose atmospheric component cannot produce these events realistically (Gebbie et al., 2007; Gebbie & Tziperman, 2009; Lopez et al., 2013). In addition to the fact that WWBs are best described as a state-dependent multiplicative forcing, it has been shown that while WWBs have a near-synoptic timescale, only the slow frequency component of these events is able to affect the ENSO cycle. This has been demonstrated for general noise forcing by Roulston & Neelin (2000), Levine & Jin (2010), and in the context of WWBs by Eisenman et al. (2005).

The causes and dynamics of WWBs are still not well understood. WWBs are associated with a rapid intensification of atmospheric convection (Nitta & Motoki, 1987) and are more likely to occur in the boreal winter and less during cold ENSO conditions (Giese & Harrison, 1991; Harrison & Vecchi, 1997). WWBs have been associated with cold surges from midlatitudes (Chu, 1988), single and paired tropical cyclones (Keen, 1982; Nitta, 1989), Rossby waves (Kiladis & Wheeler, 1995; Puy et al., 2016), and inconclusively, to the Madden Julian Oscillation (MJO; C. Zhang, 1996; Seiki & Takayabu, 2007a, 2007b; Chiodi et al., 2014; Slingo et al., 1999). WWBs in the Community Climate System Model were found comparable to observations in many aspects (Lian et al., 2018). Yet the variability of these events (Fasullo & Webster, 2000) makes it difficult to identify a unique mechanism (Lengaigne et al., 2004). It seems that the MJO may modulate the frequency and characteristics of WWBs (Seiki & Takayabu, 2007a, 2007b; Chiodi et al., 2014; Puy et al., 2016), but that the WWB mechanism is independent of the MJO. A recent work (Fu & Tziperman, 2019) finds that convective heating plays a key role in the generation of model WWBs. Furthermore, wind-induced surface heat exchange acts on a short time scale of about 2 days to dramatically amplify the model WWB winds near the peak of the event. On the other hand, it is found that radiation feedbacks (long wave and short wave) and sensible surface heat flux are not essential for the development of model WWBs.

7.3. ENSO AMPLITUDE ASYMMETRY

The 1982–1983, 1997–1998 and 2015–2016 El Niños are usually called “extreme El Niños.” Although there is no consensus on the definition of an extreme El Niño, so far there has been no La Niña event comparable to such strong El Niño events. This amplitude asymmetry between El Niño and La Niña can be featured by a positively skewed probability distribution of ENSO index (Figure 7.5) (e.g. Burgers & Stephenson, 1999; Deser & Wallace, 1987) as well as a horizontal pattern of skewness of SST anomalies (Figure 7.5). Not only the strong positive skewness over the eastern Pacific but also weak negative skewness over the western Pacific were found mainly because of a pattern asymmetry between El Niño and La Niña (e.g. Burgers & Stephenson, 1999; Takahashi et al., 2011; Dommenges et al., 2013). Such higher order moment implies nonlinearity in a tropical atmosphere-ocean coupled system or asymmetric impact of external forcing. In this section, we introduce the current hypotheses on driving mechanisms of the amplitude asymmetry (section 7.3.1) and the extreme El Niño (section 7.3.2), as well as a conceptual model to explain the amplitude asymmetry (section 7.3.3). Finally, the amplitude asymmetry of ENSO appearing in climate system models is shown (section 7.3.4).

7.3.1. Cause of Amplitude Asymmetry

Why is El Niño greater than La Niña? Since there is no strong evidence for a comparable asymmetry in an external forcing so far, it is highly likely that it is related to a nonlinear nature in tropical coupled ocean-atmosphere system, particularly in its feedbacks. “Bjerknes feedback,” referring to a positive feedback between the equatorial surface winds and zonal SST contrast between equatorial western and eastern Pacific (Bjerknes, 1966, 1969) was known as a major growing mechanism of both El Niño and La Niña. Recent studies anatomized Bjerknes feedback to figure out detailed processes, and the positive feedback on ENSO system was revealed to be quite nonlinear, especially associated with nonlinear response of atmospheric pattern to SST anomalies (Kang & Kug, 2002; Im et al., 2015). These nonlinear Bjerknes feedback processes turn out to be responsible for amplitude asymmetry of ENSO (see Figure 7.2).

One potentially important oceanic process in nonlinear Bjerknes feedback is a nonlinear dynamical heating (NDH), which indicates three-dimensional adiabatic heat flux. The NDH produces positive SST tendency over the equatorial central-to-eastern Pacific by its vertical component (An & Jin, 2004) and far eastern Pacific by its zonal and meridional components (Su et al., 2010), regardless of signs of SSTA (sea surface temperature

anomalies), and thus it enhances El Niño but suppresses La Niña (An, 2009). However, there is an unresolved issue on the actual role of each component of NDH. For example, earlier work by Zebiak and Cane (1986) and An and Jin (2004) showed that nonlinear vertical temperature advection results in the asymmetry between the amplitudes of El Niño and La Niña. Yet Su et al. (2010) found, using three different ocean reanalysis products, that nonlinear zonal and meridional advection plays a crucial role in leading to an El Niño amplitude that is larger than La Niña’s, while nonlinear vertical advection plays an opposite role, specifically over the far eastern Pacific. Moreover, the roles of nonlinear vertical temperature advection, especially during the development phase of El Niño, were inconsistent among ocean assimilation products (Su et al., 2010), and thus further analysis using an advanced assimilation data combined with higher quality observations in both space and time need to be pursued to resolve this issue.

Another nonlinear oceanic process is related to the activity of tropical instability waves (TIWs), especially over off-equatorial eastern Pacific. TIW is an intraseasonal oceanic phenomenon driven by barotropic and baroclinic instabilities, and thus relatively slowly varying El Niño and La Niña could not only modify their activity but also be influenced by them. During La Niña, the enhanced meridional SST gradient intensifies TIW activity, while during El Niño, TIW activity is suppressed (An, 2008a, 2008b; J. Yu & Liu, 2003). Therefore, strong

lateral mixing by TIW suppresses La Niña but does not influence El Niño much (Vialard et al., 2001). Large-scale ocean waves driven by ENSO-related wind stress are also responding asymmetrically. Oceanic wave response to wind stress depends on not only the wind stress itself but also thermocline depth. In particular, the equatorial Rossby wave response to the wind stress curl becomes more sensitive during El Niño compared with La Niña because of the shallow western Pacific thermocline depth during El Niño (An & Kim, 2017), which could cause amplitude asymmetry (Im et al., 2015).

In addition to oceanic nonlinear process, the atmospheric response in ENSO timescale to SSTA between El Niño and La Niña have systematic differences. The equatorial zonal wind stress response to El Niño-induced SSTA is stronger than that to La Niña-induced SSTA (Choi et al., 2013; Frauen & Dommenget, 2010; Kang & Kug, 2002). This amplitude asymmetry in the wind response is also related to its pattern asymmetry (Kang & Kug, 2002). Usually the major surface wind patch of El Niño is located further east than that of La Niña. This eastward shift is related to the nonlinearity in the response of deep convection to SSTA (Ham & Kug, 2012; Hoerling et al., 1997; Kang & Kug, 2002). Another nonlinear feedback process is a nonlinear shortwave-cloud-SST interaction (T. Li & Philander, 1996; T. Li, 1997a; Lloyd et al., 2012). This shortwave feedback depends on the atmospheric stability. Over convectively unstable regions, the shortwave surface heat flux is reduced by more con-

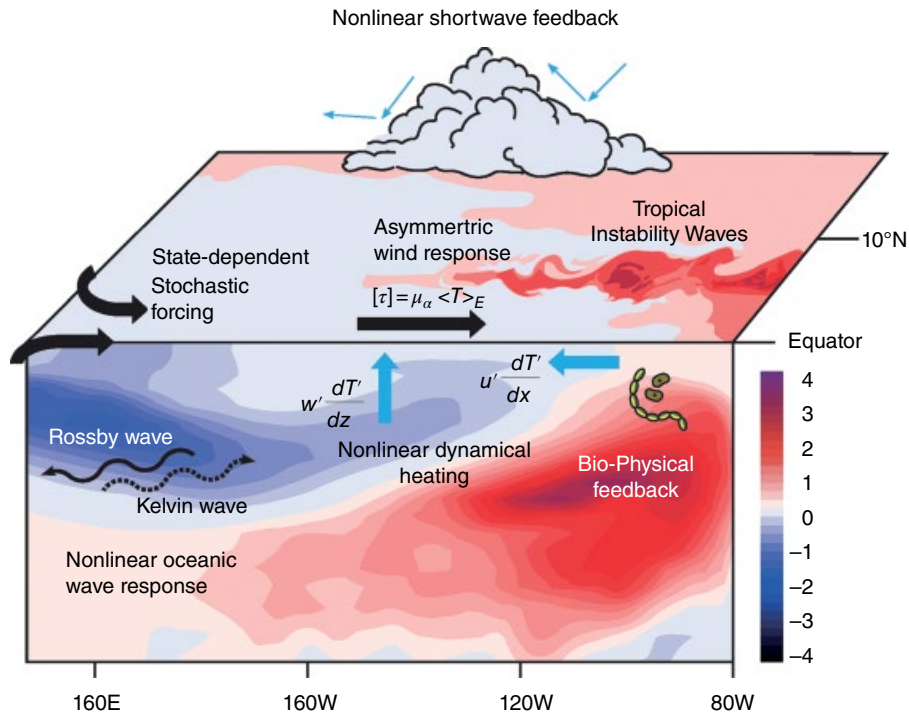


Figure 7.2 Schematic diagram for nonlinear processes responsible for asymmetric amplitude of ENSO (see text).

vective clouds associated with the increase in SSTAs, and the opposite case occurs with the decrease in SSTA. While over stable regions, the destabilizing effect on the atmospheric boundary layer due to warmer SSTA destructs the stratiform layer clouds and leads to an increase in the shortwave surface heat flux. To colder SSTA, the situation becomes opposite. Therefore, the shortwave feedback becomes either positive or negative, depending on atmospheric stability condition. Furthermore, the increase (decrease) in convective clouds associated with positive (negative) SSTA enhances (reduces) the greenhouse effect, and thus the longwave surface flux feedback is positive. Actually, the thermodynamical damping is stronger during El Niño compared to La Niña, which is mainly attributed to the difference in damping by the shortwave feedback between El Niño and La Niña (Im et al., 2015).

Finally, more active westerly wind bursts during El Niño compared with La Niña was suggested for the amplitude asymmetry (Jin et al., 2007) by enhancing a positive feedback of ENSO system during El Niño via a multiplicative noise effect (Levine & Jin, 2010). ENSO influences a supply of nutrients in ocean's surface by changing upwelling, leading to change in phytoplankton concentration; the change in phytoplankton biomass in turn affects ocean mixed layer temperature by modifying the penetration of solar radiation. During La Niña especially, phytoplankton blooming due to the enhanced nutrient supply associated with strong upwelling leads to surface warming, thereby damping La Niña. As a result, the biophysical feedback leads to amplitude asymmetry, of which efficiency is further enhanced during La Niña because of shallower mixed depth (Marzeion et al., 2005; Timmermann & Jin, 2002).

7.3.2. Extreme El Niño Formation Mechanisms

The strong El Niño events in 2015–2016, 1997–1998, and 1982–1983, referred to here as extreme El Niño, caused remarkably devastating weather and climate (floods, droughts, heat waves, and hurricanes) around the world. An extreme El Niño was anticipated in early 2014 (Tollefson, 2014), but it had failed to materialize by the end of 2014. While the scientific community was still puzzling about the cause of the aborted El Niño event in 2014, the remnants of the decaying warming in late 2014 unexpectedly reignited in February 2015 and grew into an extreme El Niño by the end of 2015.

L. Chen et al. (2016) conducted an observational analysis to reveal statistically significant different precursor signals between an extreme and a regular El Niño group. The El Niño events during 1958–2008 were separated into two groups: an extreme El Niño group and a regular El Niño group. A composite analysis showed that a

significant SSTA tendency difference between the two groups occurs during the onset phase (April–May) when the SSTA is nearly zero for both the groups. A mixed-layer heat budget analysis indicates that the SSTA tendency difference between the two groups arises primarily from the difference in zonal current anomaly (u') and associated zonal advection term. The major factors that causes the u' difference is the thermocline depth anomaly (D') in the off-equatorial western Pacific prior to the onset phase. A further diagnosis showed that the D' difference is caused by the difference in the local wind stress curl anomaly regulated by anomalous SST and precipitation over the Maritime Continent and equatorial western Pacific.

It is interesting to note that precursory D' signal in 2015's extreme El Niño was very different from that of traditional extreme El Niños such as those in 1998 and 1982 (L. Chen et al., 2017). Figure 7.3a compares the evolutions of the Niño-3 SSTA for the 2015 extreme El Niño, the traditional extreme El Niño (defined as the composite of the 1982 and 1997 events), and the regular El Niño composite. Two marked differences are worth noting. First, in contrast to the traditional extreme El Niño that started from a cold episode in the preceding year, 2015 El Niño was preceded by a weak warming peak in November 2014 (Figure 7.3a). Second, a marked turnabout of the SSTA tendency (from negative to positive) happened around February 2015.

The precondition of D' and the associated SSTA evolution differed markedly between 2015's El Niño and the traditional extreme El Niño during initial onset stage. The ocean-atmosphere system prior to the traditional extreme El Niño exhibited a La Niña state, as seen in Figure 7.3a. Equatorial easterly anomalies associated with the precursory cold anomaly caused anticyclonic wind stress curl anomalies, which built up positive upper-ocean heat content anomalies off the equator. The positive off-equatorial D' signals propagated westward as Rossby waves and became downwelling equatorial Kelvin waves after being reflected in the western boundary. The positive D' led to great thermocline and zonal advective feedbacks and thus a strong positive SSTA tendency during the initial developing stage of the traditional extreme El Niño.

In contrast, the pre-onset condition of the 2015 extreme El Niño was unfavorable for the occurrence of even a moderate El Niño event. During OND[-1], the ocean-atmosphere system possessed a weak and decaying El Niño pattern. A negative D' built up over off-equatorial western Pacific during OND[-1]. The negative D' was supposed to move to the equator in the following months, reducing the remnants of preceding positive thermocline anomalies at the equator. However, a positive D' signal unexpectedly intensified over central equatorial Pacific

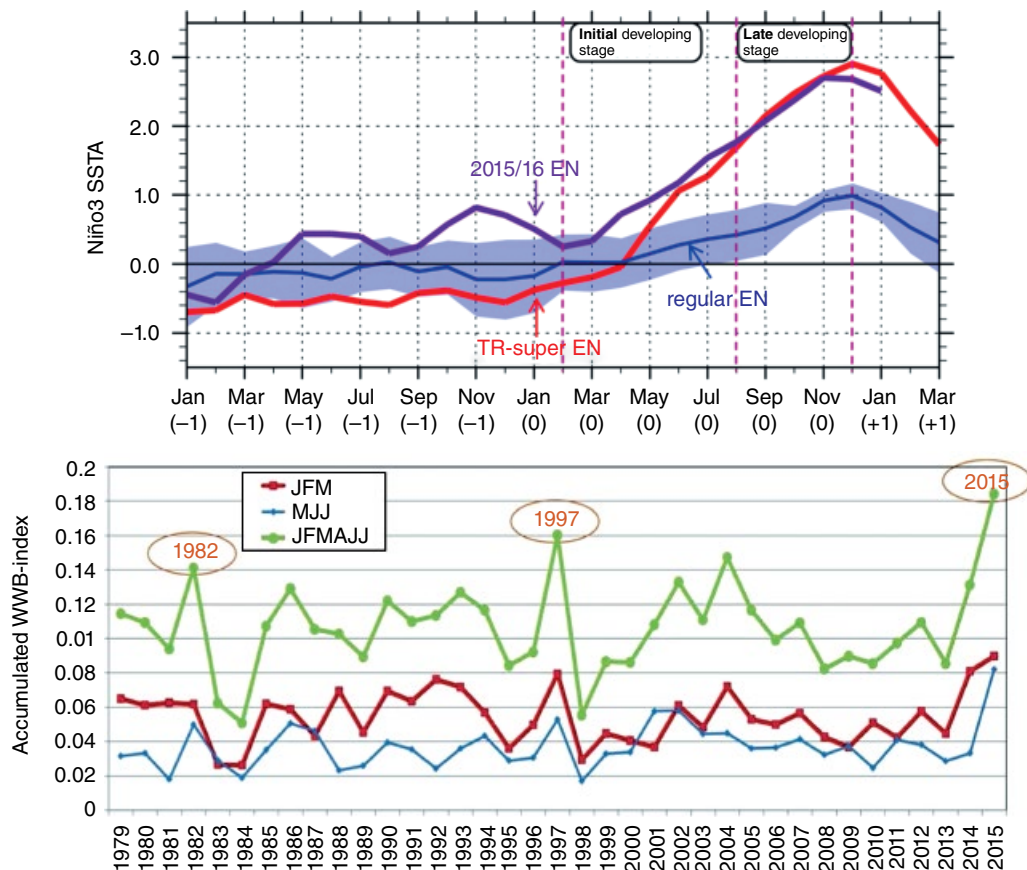


Figure 7.3 (a) Time evolution of Niño-3 SSTA. Purple line indicates the 2015–2016 El Niño, red line indicates the composite of traditional extreme EN events (i.e. 1982–1983 EN and 1997–1998 EN), and blue line indicates the composite of the regular EN events during 1980–2015 (including 1986–1987, 1987–1988, 1991–1992, 1994–1995, 2002–2003, 2004–2005, 2006–2007, and 2009–2010 ENs). The light blue shading indicates the intercase spread, which is estimated with the intercase standard deviation of the regular EN events. (b) Time series of the accumulated WWB index, which is obtained through integrating the high-frequency wind stress anomalies over (5°S – 5°N , 120 – 180°E) for January–March (JFM; red curve), May–July (MJJ; blue curve) and January–July (JFMAJJ; green curve) of each year. (Figures from L. Chen et al., 2017)

(CEP) in FM[0] and expanded into the eastern equatorial Pacific in AM[0].

The sudden emergence of this positive D' center in CEP is responsible for the turnabout of the SSTA tendency in February 2015, as clearly shown from an ocean mixed-layer heat budget. The sudden increase of D' over CEP in early 2015 was attributed to exceptional WWBs (Harrison & Vecchi, 1997; Lengaigne et al., 2004). An accumulated WWB effect was introduced by L. Chen et al. (2017) to quantitatively measure the strength of WWBs for each year. Their calculation showed that the intensity of the WWBs in early 2015 is the strongest during the past 40 years (Figure 7.3b). Oceanic general circulation model experiments further confirmed the role of the WWB in triggering the positive D' in early 2015.

In summary, the occurrence of a series of exceptionally strong WWBs in early 2015 was the major driver to flare

up a positive D' center over CEP and cause the 2015 extreme El Niño formation. The unique developing characteristic breaks our traditional view of El Niño formation, which emphasized the off-equatorial thermocline recharging process. The result suggests two routes for extreme El Niño formation (Figure 7.4). The first route is the occurrence of an exceptionally strong positive precursory D' signal in off-equatorial western Pacific. The 1997 and 1982 events are such examples. The second route is the occurrence of exceptionally strong WWBs. The formation of the 2015 extreme El Niño is such an example. While a precursory negative off-equatorial D' signal favored the occurrence of thermocline shoaling at the equator in subsequent months, such a discharging process was interrupted by the consecutive extremely strong WWBs. Thus, the 2015 episode is a shining example of the importance of WWBs. They can turn

around slow coupled dynamics and cause the generation of an extreme El Niño.

By analyzing CMIP3 and CMIP5 model outputs, Cai et al. (2014) found that the increase of extreme ENSO frequency under global warming arises from projected surface warming over the eastern equatorial Pacific that appears greater than in the surrounding ocean waters. Such a warming pattern facilitates more frequent occurrences of atmospheric convection in the eastern equatorial Pacific region. Takahashi and Dewitte (2016) and Takahashi et al. (2019) showed a bimodal probability distribution of ENSO amplitude in a Geophysical Fluid Dynamics Laboratory coupled model and a simple theoretical model. They suggested the bimodality arose from the existence of a threshold of the SSTA above which zonal wind response is nonlinearly enhanced. Recently, Cai et al. (2018) demonstrated based on CMIP5 model diagnosis that more frequent eastern Pacific-type El Niños would occur in the future warmer climate.

7.3.3. Conceptual Models to Explain Amplitude and Transition Asymmetries

The delayed action oscillator (Suarez & Schopf, 1988; Battisti & Hirst, 1989) and later recharge oscillator (F.-F. Jin, 1997a, 1997b; T. Li, 1997b) well explained an oscillatory nature of ENSO by adopting the tropical air-sea coupled feedback (Bjerknes feedback) and the slow ocean adjustment (see chapter 6 of this book). However, because

they were built on a linear dynamic framework except for a cubic term that generates a symmetric nonlinearity in the delayed action oscillator model (see Eq. 7.1), they could not explain the asymmetric features of ENSO. To compensate for this shortcoming, recent studies attempted to expand either the delayed oscillator or the recharge oscillator model to a nonlinear model by adopting the aforementioned nonlinear feedback processes (e.g. Frauen & Dommenget, 2010; Choi et al. 2013; Roberts et al., 2016; An & Kim, 2017; Timmermann et al., 2018).

The delayed oscillator model (DOM) is given by

$$\frac{\partial T}{\partial t} = -bT(t-\tau) + cT - eT^3, \tag{7.1}$$

where T represents the equatorial eastern Pacific SST anomaly; b and c indicate coefficients for the delayed negative feedback via equatorial ocean wave motions and a comprehensive simultaneous positive/negative feedback (hereafter just positive feedback because $c > 0$) via thermodynamical and dynamical air-sea coupling processes, respectively; τ represents the delay time; and e a symmetric nonlinear damping to restrict an exponential growth. Basically, b and c are responsible for the transition and growth of ENSO, respectively. In the original DOM (e.g. Battisti & Hirst, 1989), both b and c were constants regardless of T . However, by modifying b and/or c based on nonlinear Bjerknes feedback, amplitude/transition asymmetry can be produced from DOM (e.g. Choi et al.,

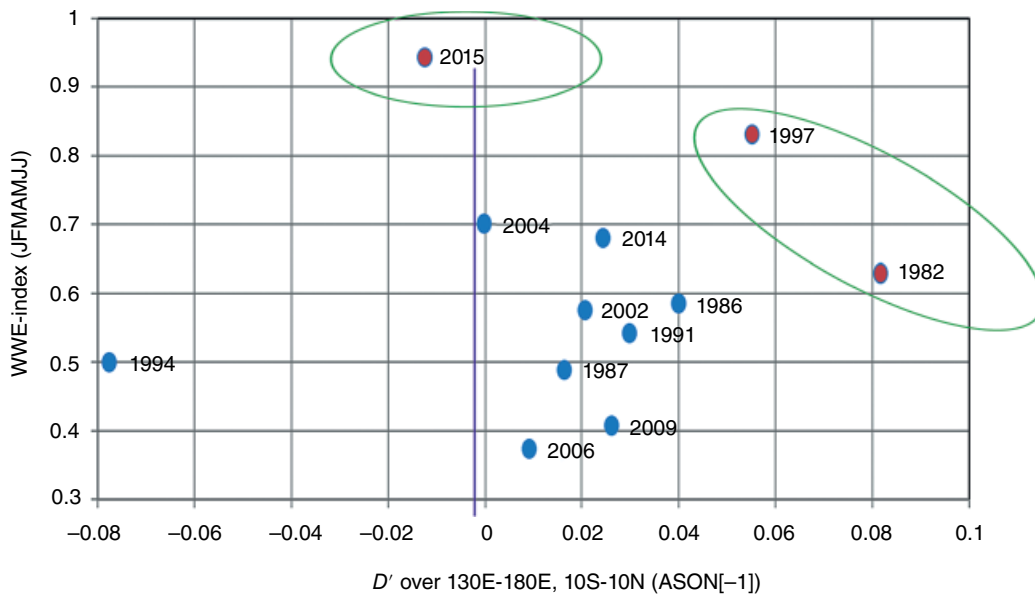


Figure 7.4 Scatter diagram for each El Niño since 1979 as a function of precursory thermocline anomaly signal (horizontal axis) and an accumulated WWB index (vertical axis). Green circle indicates two distinctive regimes for extreme El Niño formation: exceptionally strong WWBs versus exceptional strong D' signal. (Figure from L. Chen et al., 2017)

2013). A simple modification that $T(t)$ converts to $T(t) + r|T(t)|$ (Choi et al., 2013), induces DOM to be a nonlinear DOM, where r is an asymmetric factor to enhance a feedback for the positive $T(t)$ and to suppress a feedback for the negative $T(t)$ (in case of $r > 0$). More specifically, the asymmetric factor, r , has a different value depending on a modified feedback (An & Kim, 2017), such that r for a delayed negative feedback and a positive feedback are represented by r_b and r_c , respectively. As a consequence of this modification, amplifying a delayed negative feedback by a factor of $(1 + r_b)/(1 - r_b)$ ($r_b > 0$) when transitioning from El Niño to La Niña relative to the other way around results in a quick termination of El Niño; and enhancing a positive feedback by a factor of $(1 + r_c)/(1 - r_c)$ ($r_c > 0$) for the growth of El Niño relative to that of La Niña produces a positive skewness. With such modification, DOM becomes

$$\frac{\partial T}{\partial t} = -bT(t-\tau) + cT - br_b|T(t-\tau)| + cr_c|T| - eT^3 \quad (7.2)$$

Depending on what nonlinear Bjerknes feedback process is considered, r_b and r_c are determined. For a positive r (both r_b and r_c) and the corresponding parameters, the modified DOM produced a positively skewed T and a relatively fast transition from El Niño to La Niña (e.g., An & Kim, 2017; Choi et al., 2013). For example, Choi et al. (2013) focused on an asymmetrical response in the intensity of the equatorial central Pacific winds to SSTA. In addition to the wind-SST asymmetrical relationship, DiNezio & Deser (2014) stressed the asymmetrical response of subsurface ocean temperature to thermocline depth anomalies. These two nonlinear processes require both r_b and r_c to be nonzero, and thus leading to change in both amplitude and transition asymmetries of ENSO. On the other hand, asymmetry associated with the thermo-dynamical damping such as shortwave feedback requires to modify $r_c \neq 0$ and $r_b = 0$, while the asymmetry in the reflected Kelvin wave response to the wind forcing does require to modify $r_b \neq 0$ and $r_c = 0$. Therefore, the former mainly modifies ENSO amplitude asymmetry, and the latter mainly modifies ENSO transition asymmetry (An & Kim, 2017, 2018).

Not only DOM but also a recharge oscillator model (ROM) has been modified to lead an amplitude and transition asymmetries of ENSO. Conceptual differences between DOM and ROM and their relative merits are discussed in chapter 6 of this book. Linear ROM is given by (e.g. Timmermann et al., 2018)

$$dT_E/dt = I_{BJ}T_E + Fh \quad (7.3a)$$

$$dh/dt = -\varepsilon h - \alpha T_E, \quad (7.3b)$$

where T_E and h represent the equatorial eastern Pacific SSTA and zonal mean thermocline depth anomaly over an equatorial Pacific, respectively. I_{BJ} indicates the Bjerknes stability index, i.e. a collective growth/damping rate of T_E ; ε is a damping rate of h and related to ocean adjustment time scale; and the frequency is determined by $\sqrt{\alpha F}$, which is called the Wyrтки index (Lu et al., 2018). Bjerknes stability is composed of “Thermal advective damping by mean currents,” “Thermo-dynamical damping,” “Thermocline feedback,” “Zonal advection feedback,” and “Ekman feedback” (Jin et al., 2006).

As in DOM, for example, a nonlinear process on asymmetric wind response to positive and negative SSTA (e.g., Choi et al., 2013; Kang & Kug, 2002) can be applied to ROM by using the absolute value function nonlinearity. In other words, T_E is converted to $T_E + r|T_E|$. Furthermore, NDH, i.e. nonlinear oceanic thermal advection (e.g. An & Jin, 2004; Boucharel et al., 2015; Jin et al., 2003; Su et al., 2010), can be deformed by a combination of T_E and h such as $\beta_1 T_E^2 + \beta_2 T_E h$. Finally, the state-dependent noise forcing is adopted as $\sigma(1 + BT_E)\xi_t$, where $\sigma\xi(t)$ is a stochastic noise with variance and B is a positive constant (e.g. Levine & Jin, 2010). Based on above modifications, the linear ROM becomes a nonlinear ROM as follows:

$$dT_E/dt = I_{BJ}(T_E + r_{BJ}|T_E|) + Fh + \beta_1 T_E^2 + \beta_2 T_E h + \sigma(1 + B(T_E + r_B|T_E|))\xi_t, \quad (7.4a)$$

$$dh/dt = -\varepsilon h - \alpha(T_E + r_\alpha|T_E|). \quad (7.4b)$$

As in DOM, Bjerknes stability (I_{BJ}) increases by a factor of $(1 + r_{BJ})/(1 - r_{BJ})$ ($r_{BJ} > 0$) for El Niño growth relative to La Niña growth, producing a positive skewness; and Wyrтки index ($\sqrt{\alpha F}$) also increases as $\sqrt{\alpha F(1 + r_\alpha)/(1 - r_\alpha)}$ ($r_\alpha > 0$) for discharging phase relative to recharging phase, leading to a relatively fast transition from El Niño to La Niña compared to that from La Niña to El Niño. The quadratic term, $\beta_1 T_E^2$ ($\beta_1 > 0$), always produces a positive SST tendency regardless of sign of T_E , thus leading to a positive skewness. Another quadratic term, $\beta_2 T_E h$, is related to a duration asymmetry of ENSO through a quarter-cycle phase difference between T_E and h . The state-dependent noise forcing is also enhanced by a factor of $(1 + r_B)/(1 - r_B)$ ($r_B > 0$) for El Niño phase relative to La Niña phase, producing a positive skewness, where $r_B \neq r_{BJ}$ because r_B is only related to a deterministic random noise. Therefore, the nonlinear ROM obviously produces amplitude and

duration/transition asymmetries of ENSO. The aforementioned nonlinear formulas may produce somewhat similar behavior because of their mathematical similarity, but quantitative comparison of each nonlinear process has not been done yet.

7.3.4. Amplitude Asymmetry in Climate Models

Most of the Earth system models are suffering to simulate the nonlinear properties of ENSO, even though the simulated ENSO amplitude is rather agreeing with the observation (An et al., 2005a; T. Zhang & Sun, 2014). Figures 7.5a and b show the tropical Pacific skewness pattern of SSTA obtained from the observation and the multimodel ensemble (MME) of 36 CMIP5 models for a historical run, respectively. The observed SST skewness pattern features a cold tongue-like pattern of a positive skewness over eastern Pacific with its maximum at the west coast of South America; a horseshoe-like pattern of negative skewness surrounding a positive skewness; and a weak positive skewness over the subtropical northern northwestern Pacific near 130°E. SST skewness from MME is very weak compared to the observed, although the spatial pattern is somewhat similar to its counterpart of observation. Smaller skewness is clearly demonstrated in a difference map between the observation and MME (Figure 7.5c), which is very similar to the observed pattern with opposite sign. T. Zhang & Sun (2014) argued that the underestimate of ENSO asymmetry in CMIP models is caused by the weaker precipitation anomalies over the eastern Pacific and westward shift of westerly wind anomalies during El Niño. It may be related to a common bias in mean states such as the stronger trade wind, smaller warm pool size, and far westward extension of cold tongue compared to the observation (e.g., Sun et al., 2013, 2016; Zheng et al., 2012).

Figure 7.5d shows variance and skewness of the Niño-3 index obtained from the historical runs of 36 CMIP5 models and observation. The observed variance and skewness are 0.8°C^2 and 0.54, respectively, for the period of 1901–2005. Skewness indicates the normalized third order moment (An & Jin, 2004). Scatter plot of both variance and skewness computed from each model simulation spread quite widely. The spread range of variance is about $0.2\text{--}2.3^{\circ}\text{C}^2$, and the MME mean variance is 0.9, indicating that the MME mean variance is close to the observed variance. The spread range of skewness is about $-0.3\text{--}1.2$, and the MME mean skewness is 0.18. MME mean skewness is quite small compared to the observed skewness. Moreover, 9 out of 36 models produced negative skewness of the Niño-3 index, and the observed skewness is out of range of one standard deviation of model's skewness. In general, the CMIP5 model's skewness is underestimated.

There is some inconclusive evidence of a weakening of the asymmetries in the amplitude (Kohyama et al., 2018) and transition (An & Kim, 2018) of ENSO due to global warming, based on future scenario experiments of Earth system models. Dynamically, it is feasible that changes associated with global warming to the ocean stratification or to a warm pool expansion may cause such changes, but further study is needed to examine these possibilities.

7.4. ENSO EVOLUTION ASYMMETRY

El Niño and La Niña exhibit distinct asymmetry not only in the amplitude but also in the temporal evolution. Kessler (2002) noted the tendency for the equatorial Pacific Ocean to remain in a weak La Niña state for a few years and questioned the cyclic nature of ENSO. The systematic difference in the evolution of El Niño and La Niña cannot be explained by linear dynamics nor stochastic atmospheric forcing. In this section, we review the ENSO evolution asymmetry in observations and climate models (section 7.4.1) and the associated mechanisms, focusing on the nonlinearities in the tropical Pacific atmosphere and ocean (section 7.4.2) and the influences from remote tropical oceans (section 7.4.3).

7.4.1. ENSO Evolution Asymmetry in Observations and Climate Models

Both observed El Niño and La Niña tend to develop in late boreal spring-summer and peak toward the end of the calendar year. On average, El Niño terminates quickly after the mature phase and transitions into a cold phase by the following summer, whereas La Niña persists throughout the second year and reintensifies in winter (Larkin & Harrison, 2002; McPhaden & Zhang, 2009; Ohba & Ueda, 2009; Okumura & Deser, 2010; Figure 7.6). Approximately two-thirds of observed El Niño events terminate after 1 year, while nearly half of La Niña events last 2 years or longer (X. Wu et al., 2019). The asymmetric evolution of El Niño and La Niña is a robust feature of the observed ENSO throughout the past century (Okumura & Deser, 2010) and is particularly pronounced for strong ENSO events after the 1980s (McPhaden & Zhang, 2009). However, only a handful of the current and previous generations of climate models reproduce the observed ENSO evolution asymmetry (Ohba et al., 2010; Deser et al., 2012; Ohba & Watanabe, 2012; Choi et al., 2013; DiNezio et al., 2017; An & Kim, 2018). Analysis of a long control simulation of one of these models suggests that the ENSO evolution asymmetry increases with the amplitude of ENSO (Okumura et al., 2017; see section 7.3.3 for a conceptual understanding).

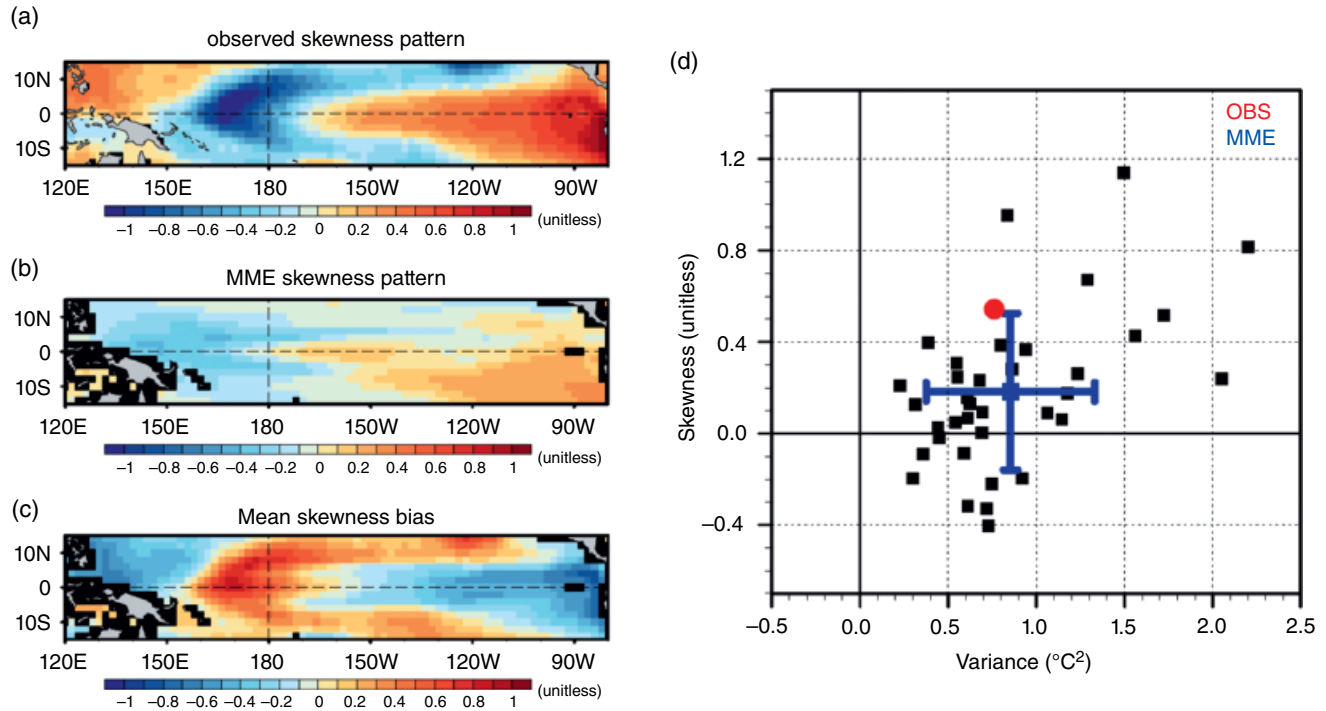


Figure 7.5 Horizontal distribution of the normalized SST skewness from (a) observation, (b) multimodel ensemble mean, and (c) their difference. (d) Scatter plot of variance (x -axis; $^{\circ}\text{C}^2$) and skewness (y -axis; normalized) of Niño-3 index (monthly-mean SST anomaly averaged over 5°S – 5°N and 150 – 90°W) for Jan. 1901–Dec. 2005 obtained from the historical run of 36 CMIP5 models (multimodel ensemble: blue rectangular), and observation (ERSSTv5: red dot). Climatological mean and linear trend were removed to calculate anomaly. Error bar indicates the range of ± 1 standard deviation.

7.4.2. Nonlinearities in the Tropical Pacific Atmosphere and Ocean

In the equatorial Pacific, surface wind anomalies drive changes in the thermocline and upwelling, which in turn affect SSTs. Early studies thus explored the atmospheric origins for the asymmetric evolution of El Niño and La Niña. Indeed, the early termination of El Niño is preceded by a rapid decay in equatorial zonal wind anomalies that begins during the mature phase (Figure 7.7). In boreal winter, when the western Pacific warm pool migrates south of the equator and the South Pacific convergence zone intensifies, the center of precipitation and zonal wind anomalies associated with El Niño shift south of the equator, hastening the discharge of the equatorial oceanic heat content and hence the event termination (Harrison & Vecchi, 1999; Vecchi, 2006; McGregor et al., 2012). The southward shift of zonal wind anomalies is pronounced for strong El Niño but inconspicuous for La Niña (Ohba and Ueda, 2009; McGregor et al., 2013). McGregor et al. (2012, 2013) discuss that weak background winds south of the equator during El Niño promote the southward shift of wind anomalies by reducing surface momentum damping.

The equatorial precipitation and zonal wind anomalies are also shifted to the east during El Niño compared to La Niña, and wind anomalies reverse the direction in the far western equatorial Pacific after the mature phase of El Niño (Figure 7.7). The zonal displacement of atmospheric anomalies is caused by nonlinear dependence of the atmospheric deep convection on SSTs (e.g. Graham & Barnett, 1987; Kang & Kug, 2002): over the eastern equatorial cold tongue, large positive SST anomalies can induce atmospheric deep convection while negative anomalies have no further effect on the normally dry conditions (Hoerling et al., 1997). Okumura et al. (2011) suggest that the eastward displacement of atmospheric anomalies makes surface winds over the western equatorial Pacific more susceptible to the delayed negative feedback from the Indian Ocean during El Niño compared to La Niña (section 7.4.3). The Indian Ocean, as well as changes in local SSTs, force atmospheric circulation anomalies over the northwest tropical Pacific during the mature-decay phase of ENSO, which act to reverse the equatorial wind anomalies (B. Wang et al., 2000; Watanabe & Jin, 2002; B. Wu et al., 2010a). These off-equatorial atmospheric circulation anomalies are also shifted eastward during El Niño compared to La Niña

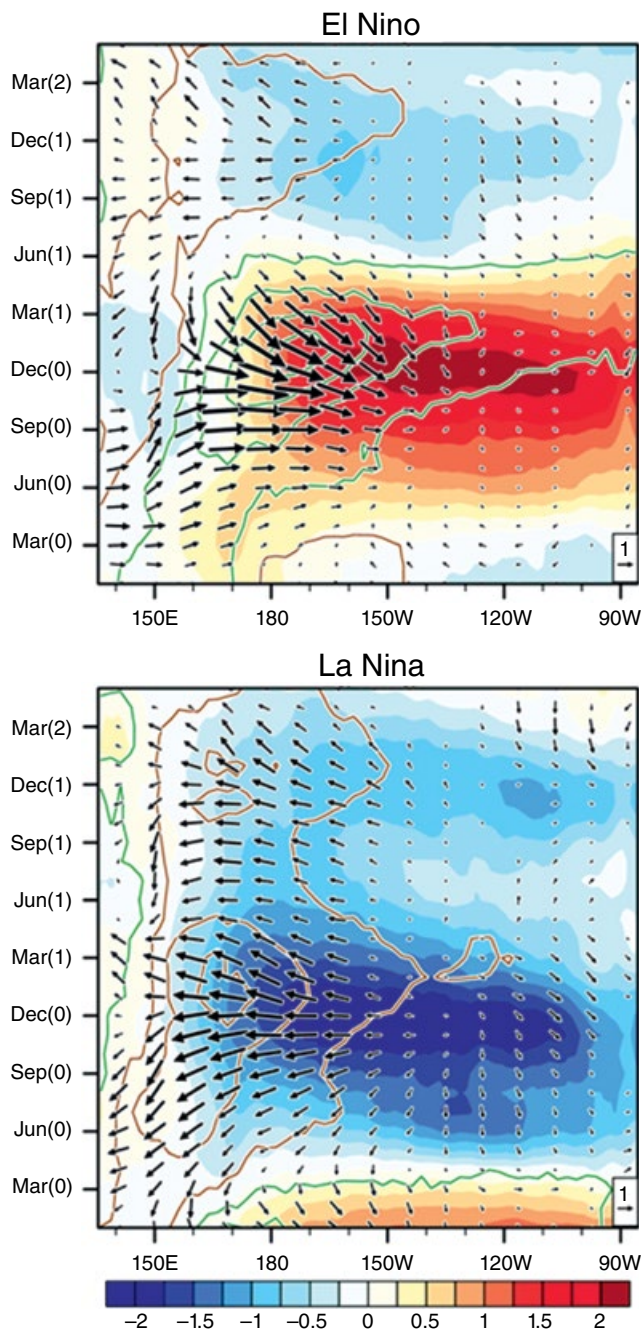


Figure 7.7 Longitude–time sections of SST ($^{\circ}\text{C}$, color shading), surface wind (m s^{-1} , vectors), and precipitation (mm day^{-1} ; positive [negative] contours in green [brown] at $\pm 1, 3, 5, \dots$) anomalies along the equator (3°S – 3°N) for strong (top) El Niño and (bottom) La Niña based on the OISST (Reynolds et al., 2002), NCEP–DOE Reanalysis II (Kanamitsu et al., 2002), and CMAP (P. Xie & Arkin, 1996) datasets for 1982–2018. The anomalies are composited for strong El Niño (1982, 1986, 1991, 1994, 1997, 2002, 2009, and 2015) and La Niña (1984, 1988, 1998, 2007, and 2010) years. The time axis runs from January(0) to May(2).

importance of different processes may be sensitive to the choice of dataset and analysis region, and further assessment will require strategic model experiments.

7.4.3. Influences from Remote Tropical Oceans

ENSO exerts significant impacts on the tropical Indian and Atlantic Oceans through atmospheric teleconnections (T. Li et al., 2003; Xie & Carton, 2004; Chang et al., 2006; Schott et al., 2009). The resultant SST changes in these remote tropical oceans, in turn, affect the atmospheric circulation and feed back to the ENSO. This so-called “capacitor effect” (Xie et al., 2009; B. Wu et al., 2009) is particularly pronounced for the Indian Ocean: during the mature-decay phase of El Niño, basinwide warming of the Indian Ocean forces an atmospheric Kelvin wave and induces easterly winds in the western equatorial Pacific, hastening the termination of El Niño (Annamalai et al., 2005; Kug & Kang, 2006; Ohba & Ueda, 2007; Yoo et al., 2010). The basinwide cooling of the Indian Ocean during the mature-decay phase of La Niña similarly forces westerly winds over the western equatorial Pacific. However, due to the westward displacement of the Pacific atmospheric anomalies during La Niña compared to El Niño, the negative feedback from the Indian Ocean is ineffective at reversing surface wind anomalies (Okumura et al., 2011).

The Indian Ocean capacitor effect itself is not the cause of the asymmetric evolution of El Niño and La Niña: it is the nonlinearity in the tropical Pacific atmosphere that makes the impact of the Indian Ocean asymmetric. Nevertheless, the basinwide SST response of the Indian Ocean is larger for El Niño than La Niña when the ENSO events concur with the Indian Ocean dipole (Hong et al., 2010), which could result in stronger negative feedback during El Niño. The inclusion of the Indian Ocean capacitor effect significantly improves the forecasts of ENSO event evolution after the mature phase only for El Niño (Ohba & Watanabe, 2012).

The delayed warming and cooling of the tropical Atlantic also act to terminate the ENSO events (Ham et al., 2013; L. Wang et al., 2017; T. Li et al., 2017), although the role in the asymmetric evolution of El Niño and La Niña is not clear (An & Kim, 2018). The capacitor effect of the Atlantic Ocean is suggested to have increased since the early 1990s in association with an upward swing of Atlantic multidecadal variability (L. Wang et al., 2017). Given the important role of inter-basin linkages in the ENSO evolution, the three tropical oceans should be viewed as a single system linked by means of the atmospheric circulation (Dommengeset & Semenov, 2006; Jansen et al., 2009; Dommengeset & Yu, 2017; see chapter 10 for further discussion on this topic).

Table 7.1 Composite mixed layer temperature anomaly budget analysis during the decaying phase of El Niño and La Niña averaged in the equatorial eastern Pacific region (5°N–5°S, 180°–80°W, unit, °C/month). “Adv” denotes advection terms, “Hflx” represents heat flux terms, “Sum” is the summation of “Adv” and “Hflx,” “sw” denotes the anomalous shortwave radiation term, and “lh” is the anomalous latent heat flux term. The values are based on the ensemble average of two ocean reanalysis datasets (GODAS and SODAv2.1.6) and two surface heat flux products (NCEPv2 and OAFflux). Adapted from M. Chen et al. (2016).

	dT'/dt	Adv	Hflx	Sum	$-u'\overline{\partial T}/\partial x$	sw'	lh'
El Niño	-0.28	-0.12	-0.20	-0.32	-0.19	-0.07	-0.14
La Niña	0.13	0.06	0.11	0.17	0.10	0.04	0.06

7.5. CONCLUSION AND DISCUSSION

In this chapter, the observed characteristics of ENSO’s irregularity and asymmetry are described, and possible physical mechanisms are discussed. These ENSO characteristics have important implications for operational forecast, as ENSO’s remote impact on global climate depends on the structure, intensity, and temporal evolution of the anomalous heating source in the tropics associated with ENSO. In spite of progress in studies of the mechanisms behind the irregularity and asymmetry of El Niño and La Niña, significant problems are still unresolved, and further studies are needed. Many current state-of-the-art coupled atmosphere-ocean general circulation models fail to capture the observed amplitude and evolution asymmetry. In this regard, future change in ENSO asymmetries revealed by global warming scenario experiments of the coupled general circulation models cannot be conclusive so far.

There are some unresolved issues regarding the asymmetry in El Niño and La Niña’s amplitude and evolution. For example, it is unclear if vertical NDH (Zebiak & Cane, 1986; An & Jin, 2004) or horizontal NDH (Su et al., 2010) plays a crucial role in leading to amplitude asymmetry. During the developing phase of El Niño, vertical NDH was especially inconsistent among ocean assimilation products (Su et al., 2010). The role of the Indian Ocean capacitor effect on a quick El Niño’s termination by inducing anomalous easterlies was questioned by M. Chen et al. (2016), who claimed that the Indian Ocean basin warming during mature El Niño wintertime events had little effect on the easterly anomalies in the equatorial western Pacific. Furthermore, the relative role and intensity of atmospheric nonlinearity (asymmetric wind response to warm and cold phase) and oceanic nonlinearities (NHD, thermocline outcropping, etc.) in producing amplitude and transition asymmetries of ENSO system have never been precisely compared. It must be very hard because as with a linear air-sea coupling, nonlinear processes in the atmosphere and ocean are interacting.

In addition to the asymmetry in their amplitude and evolution, El Niño and La Niña also exhibit a pattern asymmetry (see chapter 4 on ENSO diversity). For

example, El Niño events may be centered over either the central Pacific or the eastern Pacific, while La Niña’s cold SST pattern is typically in between these El Niño warm spots (e.g. Kug & Ham, 2011). It is not clear what mechanisms are responsible for this ENSO pattern asymmetry, although it is likely related to the amplitude and evolution asymmetry discussed above.

While simple models such as those introduced in earlier sections are a useful tool in conceptually understanding ENSO’s complicated behavior, the cause of ENSO’s amplitude asymmetry may be beyond the scope of such models. For example, most prototype ENSO models represent explicitly only one or two spatial locations, such as the eastern and western Pacific, which does not allow for amplitude asymmetry caused by pattern asymmetry. An effort is required to reveal the cause of failure of current state-of-the-art coupled general circulation models in capturing the observed amplitude, structure, and evolution asymmetry of ENSO.

ACKNOWLEDGMENTS

S.-I. An was supported by the Basic Science Research Program through the National Research Foundation of Korea (NRF-2017R1A2A2A05069383, NRF-2018R1A5A1024958) and appreciates J.-W. Kim for drawing Figure 7.5. E. Tziperman was supported by the NSF climate dynamics program, grant AGS-1826635, and by a Harvard-UTEC collaborative grant, and would like to thank the Weizmann Institute for its hospitality during parts of this work. Y. Okumura was supported by the US National Oceanic Atmosphere Administration (NA17OAR 4310149) and National Science Foundation (OCE1756883). T. Li was supported by NSFC grant 41630423, NSF grant AGS-2006553, and NOAA grant NA18OAR4310298.

REFERENCES

- Annamalai, H., Xie, S.-P., McCreary, J. P., & Murtugudde, R. (2005). Impact of Indian Ocean sea surface temperature on a developing El Niño. *Journal of Climate*, 18, 302–319. <https://doi.org/10.1175/JCLI-3268.1>

- An, S.-I. (2008a). Interannual changes in the variability of tropical Pacific instability waves. *Asia-Pacific Journal of Atmospheric Sciences*, 44, 249–258.
- An, S.-I. (2008b). Interannual variations of the tropical ocean instability wave & ENSO. *Journal of Climate*, 21, 3680–3686. <https://doi.org/10.1175/2008JCLI1701.1>
- An, S.-I. (2009). A review of interdecadal changes in the nonlinearity of the El Niño-Southern Oscillation. *Theoretical & Applied Climatology*, 97, 29–40. <https://doi.org/10.1007/s00704-008-0071-z>
- An, S.-I., Ham, Y.-G., Jin, F.-F., Kug, J.-S., & Kang, I.-S. (2005a). El Niño La Niña asymmetry in the Coupled Model Intercomparison Project simulations. *Journal of Climate*, 18, 2617–2627. <https://doi.org/10.1175/JCLI3433.1>
- An, S.-I., Hsieh, W.-W., & Jin, F.-F. (2005b). A nonlinear analysis of the ENSO cycle and its interdecadal changes. *Journal of Climate*, 18, 3229–3239. <https://doi.org/10.1175/JCLI3466.1>
- An, S.-I., & Jin, F.-F. (2000). An eigen analysis of the interdecadal changes in the structure and frequency of ENSO mode. *Geophysical Research Letters*, 27, 1573–1576.
- An, S.-I., & Jin, F.-F. (2001). Collective role of thermocline and zonal advective feedbacks in the ENSO mode. *Journal of Climate*, 14, 3421–3432.
- An, S.-I., & Jin, F.-F. (2004). Nonlinearity and asymmetry of ENSO. *Journal of Climate*, 17, 2399–2412. [https://doi.org/10.1175/1520-0442\(2004\)017<2399:NAAOE>2.0.CO;2](https://doi.org/10.1175/1520-0442(2004)017<2399:NAAOE>2.0.CO;2)
- An, S.-I., & Jin, F.-F. (2011). Linear solutions for the frequency and amplitude modulation of ENSO by the annual cycle. *Tellus*, 63, 238–243.
- An, S.-I., & Kim, J.-W. (2017). Role of nonlinear ocean dynamic response to wind on the asymmetrical transition of El Niño and La Niña. *Geophysical Research Letters*, 44, 393–400. <https://doi.org/10.1002/2016GL071971>
- An, S.-I., & Kim, J.-W. (2018). ENSO Transition asymmetry: Internal and external causes and intermodel diversity. *Geophysical Research Letters*, 45, 5095–5104. <https://doi.org/10.1029/2018GL078476>
- Battisti, D. S., & Hirst, A. C. (1989). Interannual variability in a tropical atmosphere–ocean model: Influence of the basic state, ocean geometry and nonlinearity. *Journal of the Atmospheric Sciences*, 46, 1687–1712.
- Bjerknes, J. (1966). A possible response of the atmospheric Hadley circulation to equatorial anomalies of ocean temperature. *Tellus*, 18, 820–829. <https://doi.org/10.3402/tellusa.v18i4.9712>
- Bjerknes, J. (1969). Atmospheric teleconnection from the equatorial Pacific. *Monthly Weather Review*, 97, 163–172. [https://doi.org/10.1175/1520-0493\(1969\)097<0163:ATFTEP>2.3.CO;2](https://doi.org/10.1175/1520-0493(1969)097<0163:ATFTEP>2.3.CO;2)
- Boucharel, J., Timmermann, A., Santoso, A., England, M.H., Jin, F.-F., & Balmaseda, M. A. (2015). A surface layer variance heat budget for ENSO. *Geophysical Research Letters*, 42, 3529–3537. <https://doi.org/10.1002/2015GL063843>
- Burgers, G., & Stephenson, D. B. (1999). The “normality” of El Niño. *Geophysical Research Letters*, 26, 1027–1030.
- Cai, W., et al. (2014). Increasing frequency of extreme El Niño events due to greenhouse warming. *Nature Climate Change*, 4, 111–116.
- Cai, W., Wang, G., Dewitte, B., Wu, L., Santoso, A., Takahashi, K., et al. (2018). Increased variability of eastern Pacific El Niño under greenhouse warming. *Nature*, 564, 201–206.
- Cane, M. A., Zebiak, S. E., & Dolan, S. C. (1986). Experimental forecasts of El Niño. *Nature*, 321, 827–832.
- Chang, P., Wang, B., Li, T., & Ji, L. (1994). Interactions between the seasonal cycle & the Southern Oscillation: Frequency entrainment & chaos in a coupled ocean-atmosphere model. *Geophysical Research Letters*, 21, 2817–2820.
- Chang, P., Yamagata, T., Schopf, P., Behera, S. K., Carton, J., Kessler, W. S., et al. (2006). Climate fluctuations of tropical coupled systems: The role of ocean dynamics. *Journal of Climate*, 19, 5122–5174. <https://doi.org/10.1175/JCLI3903.1>
- Chen, D. et al. (2015). Strong influence of westerly wind bursts on El Niño diversity. *Nature Geoscience*, 8, 339–345.
- Chen, L., Li, T., Behera, S. K., & Doi, T. (2016a). Distinctive precursory air–sea signals between regular and super El Niños. *Advances in Atmospheric Sciences*, 33, 996–1004.
- Chen, L., Li, T., Wang, B., & Wang, L. (2017). Formation mechanism for 2015/16 super El Niño. *Scientific Reports*, 7, 2975. [doi:10.1038/s41598-017-02926-3](https://doi.org/10.1038/s41598-017-02926-3)
- Chen, M., Li, T., Shen, X., & Wu, B. (2016b). Relative roles of dynamic and thermodynamic processes in causing evolution asymmetry between El Niño and La Niña. *Journal of Climate*, 29, 2201–2220. <https://doi.org/10.1175/JCLI-D-15-0547.1>
- Chen, M., & Li, T. (2018). Why 1986 El Niño and 2005 La Niña evolved different from a typical El Niño and La Niña. *Clim. Dyn.*, 51, 4309–4327. [doi:10.1007/s00382-017-3852-1](https://doi.org/10.1007/s00382-017-3852-1)
- Chiodi, A. M., Harrison, D. E., & Vecchi, G. A. (2014). Subseasonal atmospheric variability and El Niño waveguide warming: Observed effects of the Madden–Julian oscillation and westerly wind events. *Journal of Climate*, 27, 3619–3642.
- Choi, K. Y., Vecchi, G. A., & Wittenberg, A. T. (2013). ENSO transition, duration, and amplitude asymmetries: Role of the nonlinear wind stress coupling in a conceptual model. *Journal of Climate*, 26, 9462–9476. <https://doi.org/10.1175/JCLI-D-13-00045.1>
- Chu, P.-S. (1988). Extratropical forcing and the burst of equatorial westerlies in the western Pacific: A synoptic study. *J. Meteorol. Soc. Jpn.*, 66, 549–563.
- Deser, C., Phillips, A. S., Tomas, R. A., Okumura, Y. M., Alexander, M. A., Capotondi, A., et al. (2012). ENSO and Pacific decadal variability in the Community Climate System Model Version 4. *Journal of Climate*, 25, 2622–2651. <https://doi.org/10.1175/JCLI-D-11-00301.1>
- Deser, C., & Wallace, J. M. (1987). El Niño events & their relation to the southern oscillation: 1925–1986. *Journal of Geophysical Research: Oceans*, 92, 14189–14196.
- DiNezio, P. N., & Deser, C. (2014). Nonlinear controls on the persistence of La Niña. *Journal of Climate*, 27, 7335–7355. <https://doi.org/10.1175/JCLI-D-14-00033.1>
- DiNezio, P. N., Deser, C., Okumura, Y., & Karspeck, A. (2017). Predictability of 2-year La Niña events in a coupled general circulation model. *Climate Dynamics*, 49, 4237–4261. <https://doi.org/10.1007/s00382-017-3575-3>
- Dommenges, D., Bayr, T., & Frauen, C. (2013). Analysis of the non-linearity in the pattern and time evolution of El Niño southern oscillation. *Climate Dynamics*, 40, 2825–2847. <https://doi.org/10.1007/s00382-012-1475-0>
- Dommenges, D., & Semenov, V. (2006). Impacts of the tropical Indian and Atlantic Oceans on ENSO. *Geophysical Research Letters*, 33, L11701. <https://doi.org/10.1029/2006GL025871>

- Dommenget, D., & Yu, Y. (2016). The seasonally changing cloud feedbacks contribution to the ENSO seasonal phase-locking. *Climate Dynamics*, *47*, 3661–3672.
- Dommenget, D., & Yu, Y. (2017). The effects of remote SST forcings on ENSO dynamics, variability and diversity. *Climate Dynamics*, *49*, 2605–2624.
- Eisenman, I., Yu, L., & Tziperman, E. (2005). Westerly wind bursts: ENSO's tail rather than the dog? *Journal of Climate*, *18*, 5224–5238.
- Farrell, B. (1988). Optimal excitation of neutral Rossby waves. *Journal of the Atmospheric Sciences*, *45*, 163–172.
- Farrell, B. F., & Ioannou, P. J. (1996). Generalized stability theory. *Part I: Autonomous operators*. *Journal of the Atmospheric Sciences*, *53*, 2025–2040.
- Fasullo, J., & Webster, P. J. (2000). Atmospheric and surface variations during westerly wind bursts in the tropical western Pacific. *Quarterly Journal of the Royal Meteorological Society*, *126*, 899–924.
- Fedorov, A. V., & Philander, S. G. (2000). Is El Niño changing? *Science*, *288*, 1997–2002.
- Frauen, C., & Dommenget, D. (2010). El Niño and la Niña amplitude asymmetry caused by atmospheric feedbacks. *Geophysical Research Letters*, *37*, 1–6. <https://doi.org/10.1029/2010GL044444>
- Fu, M., & Tziperman, E. (2019). Essential ingredients to the dynamics of westerly wind bursts. *Journal of Climate*. doi: 10.1175/JCLI-D-18-0584.1
- Galanti, E., & Tziperman, E. (2000). ENSO's phase locking to the seasonal cycle in the fast-SST, fast-wave, and mixed-mode regimes. *Journal of the Atmospheric Sciences*, *57*, 2936–2950.
- Galanti, E., Tziperman, E., Harrison, M., Rosati, A., Giering, R., and Sirkes, Z. (2002). The equatorial thermocline outcropping: A seasonal control on the tropical Pacific ocean-atmosphere instability strength. *Journal of Climate*, *15*, 2721–2739.
- Gebbie, G., Eisenman, I., Wittenberg, A., & Tziperman, E. (2007). Modulation of westerly wind bursts by sea surface temperature: A semistochastic feedback for ENSO. *Journal of the Atmospheric Sciences*, *64*, 3281–3295. doi:10.1175/JAS4029.1
- Gebbie, G., & Tziperman, E. (2009). Predictability of SST-modulated westerly wind bursts. *Journal of Climate*, *22*, 3894–3909.
- Giese, B. S., & Harrison, D. E. (1991). Eastern equatorial Pacific response to three composite westerly wind types. *Journal of Geophysical Research: Oceans*, *96*, 3239–3248.
- Graham, N. E., & Barnett, T. P. (1987). Surface temperature, surface wind divergence, and convection over tropical oceans. *Science*, *238*, 657–659. <https://doi.org/10.1126/science.238.4827.657>
- Ham, Y.-G., & Kug, J.-S. (2012). How well do current climate models simulate two types of El Niño? *Climate Dynamics*, *39*, 383–398. <https://doi.org/10.1007/s00382-011-1157-3>
- Ham, Y.-G., Kug, J.-S., Park, J.-Y., & Jin, F.-F. (2013). Sea surface temperature in the north tropical Atlantic as a trigger for El Niño/Southern Oscillation events. *Nature Geoscience*, *6*, 112–116. <https://doi.org/10.1038/ngeo1686>
- Harrison, D. E., & Vecchi, G. A. (1997). Westerly wind events in the tropical Pacific, 1986–95. *Journal of Climate*, *10*, 3131–3156.
- Harrison, D. E., & Vecchi, G. A. (1999). On the termination of El Niño. *Geophysical Research Letters*, *26*, 1593–1596. <https://doi.org/10.1029/1999GL900316>
- Hayashi, M., & Watanabe, M. (2017). ENSO complexity induced by state dependence of westerly wind events. *Journal of Climate*, *30*, 3401–3420.
- Hoerling, M. P., Kumar, A., & Zhong, M. (1997). El Niño, La Niña, and the nonlinearity of their teleconnections. *Journal of Climate*, *10*, 1769–1786. [https://doi.org/10.1175/1520-0442\(1997\)010<1769:ENOLNA>2.0.CO;2](https://doi.org/10.1175/1520-0442(1997)010<1769:ENOLNA>2.0.CO;2)
- Hong, C.-C., Li, T., & Chen, Y.-C. (2010). Asymmetry of the Indian Ocean basinwide SST anomalies: Roles of ENSO & IOD. *Journal of Climate*, *23*, 3563–3576. <https://doi.org/10.1175/2010JCLI3320.1>
- Im, S.-H., An, S.-I., Kim, S. T., & Jin, F.-F. (2015). Feedback processes responsible for El Niño–La Niña amplitude asymmetry. *Geophysical Research Letters*, *42*, 5556–5563. <https://doi.org/10.1002/2015GL064853>
- Jansen, M. F., Dommenget, D., & Keenlyside, N. (2009). Tropical atmosphere-ocean interactions in a conceptual framework. *Journal of Climate*, *22*, 550–567. <https://doi.org/10.1175/2008JCLI2243.1>
- Jin, F.-F. (1997a). An equatorial ocean recharge paradigm for ENSO. *Part I: Conceptual model*. *Journal of the Atmospheric Sciences*, *54*, 811–829. [https://doi.org/10.1175/1520-0469\(1997\)054<0811:AEORPF>2.0.CO;2](https://doi.org/10.1175/1520-0469(1997)054<0811:AEORPF>2.0.CO;2)
- Jin, F.-F. (1997b). An equatorial ocean recharge paradigm for ENSO. *Part II: A stripped-down coupled model*. *Journal of the Atmospheric Sciences*, *54*, 830–847. [https://doi.org/10.1175/1520-0469\(1997\)054<0830:AEORPF>2.0.CO;2](https://doi.org/10.1175/1520-0469(1997)054<0830:AEORPF>2.0.CO;2)
- Jin, F.-F., Neelin, J. D., & Ghil, M. (1994). El Niño on the devil's staircase: Annual and subharmonic steps to chaos. *Science*, *264*, 70–72. doi: 10.1126/science.264.5155.70
- Jin, F.-F., An, S. I., Timmermann, A., & Zhao, J. (2003). Strong El Niño events and nonlinear dynamical heating. *Geophysical Research Letters*, *30*, 1–4. <https://doi.org/10.1029/2002GL016356>
- Jin, F.-F., Lin, L., Timmermann, A., & Zhao, J. (2007). Ensemble-mean dynamics of the ENSO recharge oscillator under state-dependent stochastic forcing. *Geophysical Research Letters*, *34*, 1–5. <https://doi.org/10.1029/2006GL027372>
- Kanamitsu, M., Ebisuzaki, W., Woollen, J., Yang, S.-K., Hnilo, J. J., Fiorino, M., & Potter, G. L. (2002) NCEP-DOE AMIP-II Reanalysis (R-2). *Bulletin of the American Meteorological Society*, *83*(11), 1631–1644.
- Kang, I.-S., & Kug, J.-S. (2002). El Niño and La Niña sea surface temperature anomalies: Asymmetry characteristics associated with their wind stress anomalies. *Journal of Geophysical Research: Atmospheres*, *107*, 1–10. <https://doi.org/10.1029/2001JD000393>
- Keen, R. A. (1982). The role of cross-equatorial tropical cyclone pairs in the Southern Oscillation. *Monthly Weather Review*, *110*, 1405–1416.
- Kessler, W. S. (2002). Is ENSO a cycle or a series of events? *Geophysical Research Letters*, *29*, 2125. doi:10.1029/2002GL015924
- Kessler, W. S., McPhaden, M. J., & Weickmann, K. M. (1995). Forcing of intraseasonal Kelvin waves in the equatorial

- Pacific. *Journal of Geophysical Research: Oceans*, 100, 10613–10631.
- Kiladis, G. N., & Wheeler, M. (1995). Horizontal and vertical structure of observed tropospheric equatorial Rossby waves. *Journal of Geophysical Research: Atmospheres*, 100, 22981–22997.
- Kirtman, B. P., & Schopf, P. S. (1998). Decadal variability in ENSO predictability and prediction. *Journal of Climate*, 11, 2804–2822.
- Kohyama, T., Hartmann, D. L., & Battisti, D. S. (2018). Weakening of nonlinear ENSO under global warming. *Geophysical Research Letters*, 45, 8557–8567. <https://doi.org/10.1029/2018GL079085>
- Kug, J.-S., & Ham, Y.-G. (2011). Are there two types of La Niña? *Geophysical Research Letters*, 38, L16704. [doi:10.1029/2011GL048237](https://doi.org/10.1029/2011GL048237)
- Kug, J.-S., & Kang, I.-S. (2006). Interactive feedback between ENSO and the Indian Ocean. *Journal of Climate*, 19, 1784–1801. <https://doi.org/10.1175/JCLI3660.1>
- Kug, J.-S., Jin, F.-F., Sooraj, K. P., & Kang, I.-S. (2008). State-dependent atmospheric noise associated with ENSO. *Geophysical Research Letters*, 35, L05701. [doi:10.1029/2007GL032017](https://doi.org/10.1029/2007GL032017)
- Larkin, N. K., & Harrison, D. E. (2002). ENSO warm (El Niño) and cold (La Niña) event life cycles: Ocean surface anomaly patterns, their symmetries, asymmetries, and implications. *Journal of Climate*, 15, 1118–1140. [https://doi.org/10.1175/1520-0442\(2002\)015<1118:EWENOA>2.0.CO;2](https://doi.org/10.1175/1520-0442(2002)015<1118:EWENOA>2.0.CO;2)
- Lengaigne, M., Boulanger, J. P., Menkes, C., Delecluse, P., & Slingo, J. (2004). Westerly wind events in the tropical Pacific and their influence on the coupled ocean-atmosphere system. *Earth Climate: The Ocean-Atmosphere Interaction, Geophysical Monograph*, 147, 49–69.
- Levine, A. F. Z., & Jin, F.-F. (2010). Noise-induced instability in the ENSO recharge oscillator. *Journal of the Atmospheric Sciences*, 67, 529–542. <https://doi.org/10.1175/2009JAS213.1>
- Levine, A., Jin, F.-F., & McPhaden, M. J. (2016). Extreme noise—extreme El Niño: How state-dependent noise forcing creates El Niño–La Niña asymmetry. *Journal of Climate*, 29, 5483–5499.
- Li, T. (1997a). Air–sea interactions of relevance to the ITCZ: Analysis of coupled instabilities and experiments in a hybrid coupled GCM. *Journal of the Atmospheric Sciences*, 54, 134–147.
- Li, T. (1997b). Phase transition of the El Niño–Southern Oscillation: A stationary SST mode. *Journal of the Atmospheric Sciences*, 54, 2872–2887.
- Li, T., & Philander, S.G.H., (1996). On the annual cycle of the equatorial eastern Pacific. *J. Climate*, 9, 2986–2998.
- Li, T., Wang, B., Chang, C.-P., & Zhang, Y. (2003). A theory for the Indian Ocean dipole-zonal mode. *J. Atmos. Sci.*, 60, 2119–2135.
- Li, T., Wang, B., Wu, B., Zhou, T., Chang, C.-P., & Zhang, R. (2017). Theories on formation of an anomalous anticyclone in western North Pacific during El Niño: A review. *Journal of Meteorological Research*, 31, 987–1006. [doi:10.1007/s13351-017-7147-6](https://doi.org/10.1007/s13351-017-7147-6)
- Li, Y., Lu, R., & Dong, B. (2007). The ENSO–Asian monsoon interaction in a coupled ocean-atmosphere GCM. *Journal of Climate*, 20, 5164–5177.
- Lian, T., Tang, Y., Zhou, L., Islam, S. U., Zhang, C., Li, X., & Ling, Z. (2018). Westerly wind bursts simulated in CAM4 and CCSM4. *Climate Dynamics*, 50, 1353–1371.
- Lloyd, J., Guilyardi, E., & Weller, H. (2012a). The role of atmosphere feedbacks during ENSO in the CMIP3 models. *Part III: The shortwave flux feedback. Journal of Climate*, 25, 4275–4293.
- Lloyd, J., Guilyardi, E., & Weller, H. (2012b). The role of atmosphere feedbacks during ENSO in the CMIP3 models. *Part III: The shortwave flux feedback. Journal of Climate*, 25, 4275–4293. <https://doi.org/10.1175/JCLI-D-11-00178.1>
- Lopez, H., Kirtman, B. P., Tziperman, E., & Gebbie, J. (2013). Impact of interactive westerly wind bursts on CCSM3. *Dynamics of Atmospheres and Oceans*, 59, 24–51.
- Lorenz, E. N. (1963). Deterministic nonperiodic flow. *Journal of the Atmospheric Sciences*, 20, 130–141.
- Lu, B., Jin, F.-F., and Ren, H.-L. (2018) A coupled dynamic index for ENSO periodicity. *Journal of Climate*, 31, 2361–2376.
- Marzeion, B., Timmermann, A., Murtugudde, R., & Jin, F.-F. (2005). Biophysical feedbacks in the tropical Pacific. *Journal of Climate*, 18, 58–70. <https://doi.org/10.1175/JCLI3261.1>
- McGregor, S., Timmermann, A., Schneider, N., Stuecker, M. F., & England, M. H. (2012). The effect of the South Pacific convergence zone on the termination of El Niño events and the meridional asymmetry of ENSO. *Journal of Climate*, 25, 5566–5586. <http://doi.org/10.1175/JCLI-D-11-00332.1>
- McGregor, S., Ramesh, N., Spence, P., England, M. H., McPhaden, M. J., & Santoso, A. (2013). Meridional movement of wind anomalies during ENSO events and their role in event termination. *Geophysical Research Letters*, 40, 749–754. <https://doi.org/10.1002/grl.50136>
- McPhaden, M. J., Bahr, F., Du Penhoat, Y., Firing, E., Hayes, S. P., Niiler, P. P., et al. (1992). The response of the western equatorial Pacific Ocean to westerly wind bursts during November 1989 to January 1990. *Journal of Geophysical Research: Oceans*, 97, 14289–14303.
- McPhaden, M. J., & Zhang, X. (2009). Asymmetry in zonal phase propagation of ENSO sea surface temperature anomalies. *Geophysical Research Letters*, 36, L13703. <https://doi.org/10.1029/2009GL038774>
- Moore, A. M., & Kleeman, R. (1999). Stochastic forcing of ENSO by the intraseasonal oscillation. *Journal of Climate*, 12, 1199–1220.
- Nitta, T. (1989). Development of a twin cyclone and westerly bursts during the initial phase of the 1986–87 El Niño. *Journal of the Meteorological Society of Japan. Ser. II*, 67, 677–681.
- Nitta, T., & Motoki, T. (1987). Abrupt enhancement of convective activity and low-level westerly burst during the onset phase of the 1986–87 El Niño. *Journal of the Meteorological Society of Japan. Ser. II*, 65, 497–506.
- Ohba, M., & Ueda, H. (2007). An impact of SST anomalies in the Indian Ocean in acceleration of the El Niño to La Niña transition. *Journal of the Meteorological Society of Japan*, 85, 335–348. <https://doi.org/10.2151/jmsj.85.335>
- Ohba, M., & Ueda, H. (2009). Role of nonlinear atmospheric response to SST on the asymmetric transition process of ENSO. *Journal of Climate*, 22, 177–192. <https://doi.org/10.1175/2008JCLI2334.1>

- Ohba, M., & Watanabe, M. (2012). Role of the Indo-Pacific interbasin coupling in predicting asymmetric ENSO transition and duration. *Journal of Climate*, *25*, 3321–3335. <https://doi.org/10.1175/JCLI-D-11-00409.1>
- Ohba, M., Nohara, D., & Ueda, H. (2010). Simulation of asymmetric ENSO transition in the WCRP CMIP3 multimodel experiments. *Journal of Climate*, *23*, 6051–6067. <https://doi.org/10.1175/2010JCLI3608.1>
- Okumura, Y. M., & Deser, C. (2010). Asymmetry in the duration of El Niño and La Niña. *Journal of Climate*, *23*, 5826–5843. <https://doi.org/10.1175/2010JCLI3592.1>
- Okumura, Y. M., Ohba, M., Deser, C., & Ueda, H. (2011). A proposed mechanism for the asymmetric duration of El Niño and La Niña. *Journal of Climate*, *24*, 3822–3829. <https://doi.org/10.1175/2011JCLI3999.1>
- Okumura, Y. M., Sun, T., & Wu, X. (2017). Asymmetric modulation of El Niño and La Niña and the linkage to tropical Pacific decadal variability. *Journal of Climate*, *30*, 4705–4733. <https://doi.org/10.1175/JCLI-D-16-0680.1>
- Ott, E. (2002). *Chaos in dynamical systems*. Cambridge University Press.
- Penland, C., & Sardeshmukh, P. D. (1995). The optimal growth of tropical sea surface temperature anomalies. *Journal of Climate*, *8*, 1999–2024.
- Perez, C. L., Moore, A. M., Zavala-Garay, J., & Kleeman, R. (2005). A comparison of the influence of additive and multiplicative stochastic forcing on a coupled model of ENSO. *Journal of Climate*, *18*, 5066–5085.
- Puy, M., Vialard, J., Lengaigne, M., & Guilyardi, E. (2016). Modulation of equatorial Pacific westerly/easterly wind events by the Madden–Julian oscillation and convectively-coupled Rossby waves. *Climate Dynamics*, *46*, 2155–2178.
- Reynolds, R. W., Rayner, N. A., Smith, T. M., Stokes, D. C., & Wang, W. (2002). An improved in situ and satellite SST analysis for climate. *Journal of Climate*, *15*, 1609–1625.
- Rong, X., Zhang, R., Li, T., & Su, J. (2011). Upscale feedback of high-frequency winds to ENSO. *Q. J. R. Meteorol. Soc.*, *137*, 894–907.
- Roulston, M. S., & Neelin, J. D. (2000). The response of an ENSO model to climate noise, weather noise and intraseasonal forcing. *Geophysical Research Letters*, *27*, 3723–3726.
- Samelson, R. M., & Tziperman, E. (2001). Instability of the chaotic ENSO: The growth-phase predictability barrier. *Journal of the Atmospheric Sciences*, *58*, 3613–3625.
- Schott, F. A., Xie, S.-P., & McCreary, J. P. (2009). Indian Ocean circulation and climate variability. *Reviews of Geophysics*, *47*, RG1002. <https://doi.org/10.1029/2007RG000245>
- Seiki, A., & Takayabu, Y. N. (2007a). Westerly wind bursts and their relationship with intraseasonal variations and ENSO. Part II: Energetics over the western and central Pacific. *Monthly Weather Review*, *135*, 3346–3361.
- Seiki, A., & Takayabu, Y. N. (2007b). Westerly wind bursts and their relationship with intraseasonal variations and ENSO. Part I: Statistics. *Monthly Weather Review*, *135*, 3325–3345.
- Slingo, J. M., Rowell, D. P., Sperber, K. R., & Nortley, F. (1999). On the predictability of the interannual behavior of the Madden–Julian oscillation and its relationship with El Niño. *Quart. J. Roy. Meteor. Soc.*, *125*, 583–609.
- Stein, K., Schneider, N., Timmermann, A., & Jin, F.-F. (2010). Seasonal synchronization of ENSO events in a linear stochastic model. *Journal of Climate*, *23*, 5629–5643.
- Stein, K., Timmermann, A., & Schneider, N. (2011). Phase synchronization of the El Niño–Southern oscillation with the annual cycle. *Physical Review Letters*, *107*, 128501.
- Stone, L., Saparin, P. I., Huppert, A., & Price, C. (1998). El Niño chaos: The role of noise and stochastic resonance on the ENSO cycle. *Geophysical Research Letters*, *25*, 175–178.
- Strogatz, S. (1994). *Nonlinear dynamics and chaos*. Westview Press.
- Stuecker, M. F., Timmermann, A., Jin, F. F., McGregor, S., & Ren, H. L. (2013). A combination mode of the annual cycle and the El Niño/Southern Oscillation. *Nat. Geosci.*, *6*, 540–544.
- Su, J., Zhang, R., Li, T., Rong, X., Kug, J.-S., & Hong, C. C. (2010). Causes of the El Niño & La Niña amplitude asymmetry in the equatorial Eastern Pacific. *Journal of Climate*, *23*, 605–617. <https://doi.org/10.1175/2009JCLI2894.1>
- Suarez, M. J., & Schopf, P. S. (1988). A delayed action oscillator for ENSO. *Journal of the Atmospheric Sciences*, *45*, 3283–3287.
- Sun, Y., Sun, D. Z., Wu, L., & Wang, F. (2013). Western Pacific warm pool and ENSO asymmetry in CMIP3 models. *Advances in Atmospheric Sciences*, *30*, 940–953. <https://doi.org/10.1007/s00376-012-2161-1>
- Sun, Y., Wang, F., & Sun, D. Z. (2016). Weak ENSO asymmetry due to weak nonlinear air–sea interaction in CMIP5 climate models. *Advances in Atmospheric Sciences*, *33*, 352–364. <https://doi.org/10.1007/s00376-015-5018-6>
- Takahashi, K., & Dewitte, B. (2016). Strong and moderate nonlinear El Niño regimes. *Climate Dynamics*, *46*, 1627–1645.
- Takahashi, K., Karamperidou, C., & Dewitte, B. (2019). A theoretical model of strong and moderate El Niño regimes. *Climate Dynamics*, *52*, 7477–7493.
- Takahashi, K., Montecinos, A., Goubanova, K., Dewitte, B. (2011). ENSO regimes: Reinterpreting the canonical and Modoki El Niño. *Geophysical Research Letters*, *38*, L10704. <https://doi.org/10.1029/2011GL047364>
- Timmermann, A., & Jin, F.-F. (2002). Phytoplankton influences on tropical climate. *Geophysical Research Letters*, *29*, 19-1–19-4. <https://doi.org/10.1029/2002GL015434>
- Timmermann, A., An, S.-I., Kug, J.-S., Jin, F.-F., Cai, W., Capotondi, A., et al. (2018). El Niño–Southern Oscillation complexity. *Nature*, *559*, 535–545. <https://doi.org/10.1038/s41586-018-0252-6>
- Tollefson, J. (2014). El Niño tests forecasters. *Nature*, *508*, 20–21.
- Tziperman, E., & Yu, L. (2007). Quantifying the dependence of westerly wind bursts on the large-scale tropical Pacific SST. *Journal of Climate*, *20*, 2760–2768.
- Tziperman, E., Stone, L., Cane, M. A., & Jarosh, H. (1994). El Niño chaos: Overlapping of resonances between the seasonal cycle and the Pacific ocean–atmosphere oscillator. *Science*, *264*, 72–74.
- Tziperman, E., Cane, M. A., & Zebiak, S. E. (1995). Irregularity and locking to the seasonal cycle in an ENSO prediction model as explained by the quasi-periodicity route to chaos. *Journal of the Atmospheric Sciences*, *52*, 293–306.

- Tziperman, E., Zebiak, S. E., & Cane, M. A. (1997). Mechanisms of seasonal-ENSO interaction. *Journal of the Atmospheric Sciences*, *54*, 61–71.
- Vecchi, G. A. (2006). The termination of the 1997/98 El Niño. *Part II: Mechanisms of atmospheric change. Journal of Climate*, *19*, 2647–2664. <https://doi.org/10.1175/JCLI3780.1>
- Verbickas, S. (1998). Westerly wind bursts in the tropical Pacific. *Weather*, *53*, 282–284.
- Vialard, J., Menkes, C., Boulanger, J.-P., Delecluse, P., Guilyardi, E., McPhaden, M. J., & Madec, G. (2001). A model study of oceanic mechanisms affecting equatorial Pacific sea surface temperature during the 1997–98 El Niño. *Journal of Physical Oceanography*, *31*, 1649–1675. [https://doi.org/10.1175/1520-0485\(2001\)031<1649](https://doi.org/10.1175/1520-0485(2001)031<1649)
- Wang, B., Wu, R., & Lukas, R. (1999). Roles of the western North Pacific wind variation in thermocline adjustment and ENSO phase transition. *J. Meteor. Soc. Japan*, *77*, 1–16.
- Wang, B., Wu, R., Lukas, R., & An, S.-I. (2001). A possible mechanism for ENSO turnabout. In IAP/Academia Sinica (Ed.), *Dynamics of atmospheric general circulation and climate* (pp. 552–578). China Meteorological Press.
- Wang, B., Wu, R., & Fu, X. (2000). Pacific-East Asian teleconnection: How does ENSO affect East Asian climate? *Journal of Climate*, *13*, 1517–1536. [https://doi.org/10.1175/1520-0442\(2000\)013<1517:PEATHD>2.0.CO;2](https://doi.org/10.1175/1520-0442(2000)013<1517:PEATHD>2.0.CO;2)
- Wang, L., Yu, J.-Y., & Paek, H. (2017). Enhanced biennial variability in the Pacific due to Atlantic capacitor effect. *Nature Communications*, *8*, 1–7. <https://doi.org/10.1038/ncomms14887>
- Watanabe, M., & Jin, F.-F. (2002). Role of Indian Ocean warming in the development of Philippine Sea anticyclone during ENSO. *Geophysical Research Letters*, *29*, 1478. <https://doi.org/10.1029/2001GL014318>
- Wu, B., Zhou, T., & Li, T. (2009). Seasonally evolving dominant interannual variability mode over the East Asia. *Journal of Climate*, *22*, 2992–3005.
- Wu, B., Li, T., & Zhou, T. (2010a). Relative contributions of the Indian Ocean and local SST anomalies to the maintenance of the western North Pacific anomalous anticyclone during the El Niño decaying summer. *Journal of Climate*, *23*, 2974–2986.
- Wu, B., Li, T., & Zhou, T. (2010b). Asymmetry of atmospheric circulation anomalies over the western North Pacific between El Niño and La Niña. *Journal of Climate*, *23*, 4807–4822. <https://doi.org/10.1175/2010JCLI3222.1>
- Wu, X., Okumura, Y. M., & DiNezio, P. (2019). What controls the duration of El Niño and La Niña events? *Journal of Climate*, *32*, 5941–5965.
- Xie, P., and Arkin, P. A. (1996). Analyses of global monthly precipitation using gauge observations, satellite estimates, and numerical model predictions. *Journal of Climate*, *9*, 840–858.
- Xie, S.-P., & Carton, J. A. (2004). Tropical Atlantic variability: Patterns, mechanisms, and impacts. *Earth Climate: The Ocean-Atmosphere Interaction, Geophysical Monograph*, *147*, 121–142.
- Xie, S.-P., Hu, K., Hafner, J., Tokinaga, H., Du, Y., Huang, G., & Sampe, T. (2009). Indian Ocean capacitor effect on Indo-Western Pacific climate during the summer following El Niño. *Journal of Climate*, *22*, 730–747. <https://doi.org/10.1175/2008JCLI2544.1>
- Yoo, S.-H., Fasullo, J., Yang, S., & Ho, C.-H. (2010). On the relationship between Indian Ocean sea surface temperature and the transition from El Niño to La Niña. *Journal of Geophysical Research: Atmospheres*, *115*, D15114. <https://doi.org/10.1029/2009JD012978>
- Yu, J. Y., & Liu, W. T. (2003). A linear relationship between ENSO intensity and tropical instability wave activity in the eastern Pacific Ocean. *Geophysical Research Letters*, *30*, 3–6. doi:10.1029/2003GL017176
- Yu, L., Weller, R. A., & Liu, W. T. (2003). Case analysis of a role of ENSO in regulating the generation of westerly wind bursts in the western equatorial Pacific. *Journal of Geophysical Research: Oceans*, *108*, 3128. doi:10.1029/2002JC001498
- Zebiak, S. E., & Cane, M. A. (1987). A Model El Niño–Southern Oscillation. *Monthly Weather Review*, *115*, 2262–2278.
- Zhang, C. (1996). Atmospheric intraseasonal variability at the surface in the tropical western Pacific Ocean. *Journal of the Atmospheric Sciences*, *53*, 739–758.
- Zhang, T., & Sun, D. Z. (2014). ENSO asymmetry in CMIP5 models. *Journal of Climate*, *27*, 4070–4093. <https://doi.org/10.1175/JCLI-D-13-00454.1>
- Zheng, Y., Lin, J. L., & Shinoda, T. (2012). *The equatorial Pacific cold tongue simulated by IPCC AR4 coupled GCMs: Upper ocean heat budget and feedback analysis*. *Journal of Geophysical Research: Oceans*, *117*. <https://doi.org/10.1029/2011JC007746>